Received: 4 January 2019 | Revised: 18 April 2019 | Accepted: 21 April 2019

DOI: 10.1002/wcms.1419

ADVANCED REVIEW

WIREs COMPUTATIONAL MOLECULAR SCIENCE WILEY

Recent advances in quantum-mechanical molecular dynamics simulations of proton transfer mechanism in various water-based environments

Aditya W. Sakti[1] | **Yoshifumi Nishimura**[2] | **Hiromi Nakai**[1,2,3]

[1]Element Strategy Initiative for Catalysts and Batteries (ESICB), Kyoto University, Kyoto, Japan

[2]Waseda Research Institute for Science and Engineering (WISE), Waseda University, Tokyo, Japan

[3]Department of Chemistry and Biochemistry, School of Advanced Science and Engineering, Waseda University, Tokyo, Japan

Correspondence
Hiromi Nakai, Waseda Research Institute for Science and Engineering (WISE), Waseda University, Tokyo 169-8555, Japan.
Email: nakai@waseda.jp

Funding information
Ministry of Education, Culture, Sports, Science, and Technology (MEXT), Japan, Grant/Award Number: KAKENHI 15K13629; Japan Society for the Promotion of Science, Grant/Award Number: KAKENHI JP26248009

Abstract

Proton transfer in water-based environments occurs because of hydrogen-bond interaction. There are many interesting physicochemical phenomena in this field, causing fast structural diffusion of hydronium and hydroxide ions. During the last few decades, to support experimental observations and measurements, quantum-mechanical molecular dynamics (QMMD) simulations with reasonable accuracy and efficiency have significantly unraveled structural, energetic, and dynamical properties of excess proton in aqueous environments. This review summarizes the state-of-the-art QMMD studies of proton transfer processes in aqueous solutions and complex systems including bulk liquid water, ice phases, and confined water in nanochannel/nanoporous materials as well as reports on CO_2 scrubbing by amine-based chemical absorption.

This article is categorized under:

Structure and Mechanism > Reaction Mechanisms and Catalysis

Molecular and Statistical Mechanics > Molecular Dynamics and Monte-Carlo Methods

Electronic Structure Theory > Semiempirical Electronic Structure Methods

Theoretical and Physical Chemistry > Reaction Dynamics and Kinetics

KEYWORDS

density functional tight binding method, divide and conquer method, hydrogen bond, proton transfer, quantum-mechanical molecular dynamics

1 | INTRODUCTION

Proton transfer (PT) is the crucial trigger for functionalization of various materials and biological systems.[1–5] The PT process has received considerable attention at the fundamental level in order to interpret the remarkably fast proton diffusivity in the hydrogen-bond (H-bond) network. Since the pioneering description of proton hopping was proposed more than 200 years ago,[6] which is referred to as structural diffusion or the Grotthuss mechanism, the contribution of water's ionic ingredients—hydronium (H_3O^+) and hydroxide (OH^-) ions—to PT has been widely investigated.[7–12] Owing to a wide variety of chemical environments and the insufficient and controversial information about molecular mechanisms, gaining deeper insights on PT events is required.

Molecular dynamics (MD) simulation is an effective computational tool that enables tracking of atomic/molecular motions and analyzing the associated microscopic properties with qualitative and quantitative accuracy. With respect to PT, theoretical

information has been utilized for complementing experimental research, in which the issues related to measurement methods are difficult to resolve. Simulation of PT events requires MD techniques with several capabilities including appropriate treatment of covalent bond formation/cleavage for structural diffusion, reasonable computational efficiency for sufficient sampling, and concurrency of multiple proton hopping in a physically rational model system.

The parameterized reactive force field (RFF)[13–17] is one of the practical approaches for describing chemical reactions in large molecular systems. The RFF potentials specifically adjusted to study hydrated protons have been developed and applied to MD simulation of an excess proton in a water system.[18–24] Among the RFF approaches, the most popular method for revealing mechanistic details and elucidating structural and dynamical properties of the PT process is the multiple empirical valence bond (MS-EVB).[25–27] The application of MS-EVB to examine proton dynamics has been investigated in diverse model systems ranging from H_3O^+ [28–45] and OH^- [41,46] diffusion in bulk water, water–ice interface,[47] and confined water environment[48–50] to metal surfaces.[51,52] The deliberate fitting of empirical parameters for achieving improved accuracy may be a lengthy task before starting MD simulations, thereby limiting the applicability of MS-EVB over a broad range of systems.

In this review, we focus on the recent progress in computational studies related to the PT process by ab initio molecular dynamics (AIMD).[53–55] The so-called Born–Oppenheimer molecular dynamics (BOMD) and Car–Parrinello MD[56] are two common approaches in AIMD, in which density functional theory (DFT)[57–59] is typically adopted as a solver of the electronic structure problem. Although the simulations of large systems are limited because of expensive computational requirements, AIMD is highly appreciated in terms of general applicability across the periodic table and explicit incorporation of polarization and charge transfer effects.

The numerous applications of AIMD have been widely conducted and reported in order to clarify the diffusion of H_3O^+ and OH^- ions in aqueous solutions.[9–12,53–55] Instead of repeating reported literature, this review emphases on some advances and challenges in the simulation of water's ionic species in bulk systems utilizing either sophisticated or approximated DFT. To capture the dynamics of ubiquitous PT processes, a full QM method is essential, thus MD simulations with a hybrid quantum mechanical/molecular mechanics (QM/MM) approach are not discussed in the present review. Subsequently, we review theoretical results of PT events in ice for emphasizing the difference in diffusion behavior of liquid and solid phases. Following the discussion about structural and dynamical characteristics of the proton in a system constituting only water molecules, the importance of PT in more complex systems is presented. As representative examples, we briefly account for the features of proton dynamics of water confined in nanosized hydrophobic channels and the key roles of the proton in the chemistry of CO_2 capture.

2 | HYDRONIUM AND HYDROXIDE ION DIFFUSIONS IN BULK WATER

After the initial pilot studies by Tuckerman et al.,[60–62] many fundamental aspects of H_3O^+ and OH^- diffusion in the liquid phase of water have been accumulated by DFT-based AIMD simulations. The following are notable insights about the molecular mechanism involving the H_3O^+ ion: solvation structure of Zundel ($H_5O_2^+$)[63] and Eigen ($H_9O_4^+$)[64] cation species,[65–67] validation of the PT process through interconversion of the two above-mentioned protonated water complexes,[7,68–70] concept of proton rattling[65,71–73] often termed as special pair dance,[70] and coupling of multiple PT events in the concerted manner.[74,75] The corresponding mechanisms for OH^- species include coordination patterns of the hydrated structure[71,76–80] and plausibility of the mechanism with a dynamical interplay between three- and four-fold structure motifs[10,11,71,76–82] in comparison to other mechanisms supposing mirror image or static solvation complexes individually.[83–85] Moreover, the influence of nuclear quantum effects on diffusion properties have been addressed.[68,76,86–90]

One important direction of the study on PT in aqueous solution is to describe accurate trajectories with high-level electronic structure methods. Several benchmarks of pure liquid water for DFT functionals beyond the commonly employed generalized gradient approximation (GGA) and for wave-function-based approaches[91–99] can be explained by their performance on describing a quantitative illustration of PT events because the H-bond structure is closely linked with the structural diffusion. Currently, the highest quality proton dynamics is obtained at the PBE0-TS level,[100] namely the hybrid PBE0 functional[101,102] combined with the Tkatchenko–Scheffler (TS) dispersion correction scheme.[103] Compensating deficiencies of GGA functionals for relatively poor molecular polarizability, H-bond strength, and underestimation tendency of liquid density attributed to the lack of long-range van der Waals forces[91,104,105] leads to a satisfactory agreement of calculated diffusion coefficients with experimental ones, as shown in Table 1. Furthermore, the simulation has provided new perspectives that approximately halved OH^- diffusion speed with respect to that of H_3O^+ is caused by unfavorable correlation of the fourfold

TABLE 1 H_3O^+ and OH^- diffusion constants (in $Å^2$/ps) and their ratios estimated from various AIMD simulations

Method	Basis set/parameter	N_{water}	$D(H_3O^+)$	$D(OH^-)$	$D(H_3O^+)/D(OH^-)$
PW91[106]	Plane wave	32	0.32[a]	1.85[a]	0.18
BLYP[107,108]	Plane wave	32	0.28[a]	0.19[a]	1.47
HCTH[109]	Plane wave	32	0.33[a]	0.04[a]	7.39
PBE[101]	Plane wave	64	1.08[b]	1.82[b]	0.59
PBE-TS[101,103]	Plane wave	64	1.28[b]	0.83[b]	1.54
PBE0-TS[101–103]	Plane wave	64	0.83[b]	0.37[b]	2.24
DFTB[110,111]	mio,[c] mio-IBI-BLYP[d]	523	0.91[c]	0.67[d]	1.36
Experimental (H_2O)			0.94[e]	0.52[e]	1.80[e]
Experimental (D_2O)			0.67[e]	0.31[e]	2.15[e]

Abbreviation: BLYP, Becke-Lee-Yang-Parr.
Experimental data are shown for comparison.
[a]Reference 10 (production runs: 20–50 ps).
[b]Reference 100 (production runs: 14–55 ps).
[c]Reference 112 (production runs: 20 ps).
[d]Reference 113 (production runs: 40 ps).
[e]Reference 114.

hypercoordinated solvation structure with simultaneous proton hopping.[100,115] Note that encouragement of the concerted PT process in an aqueous environment is recently revisited.[116]

Despite a good agreement of the estimated diffusion constants, one should also note that the use of plane wave basis may also lead to various discrepancies, namely, overstructured radial distribution functions (RDFs) that leads to a more rigid H-bond network and slow water diffusivity.[117] Earlier study also pointed out the needs of a larger basis set TZV2P when the meta-GGA functionals were employed for improving the RDFs and self-diffusion of water.[94,118]

The other intriguing progress is to resolve the issue of system size by using computationally cost-effective quantum chemical methods. The implementation of a scalable algorithm for DFT-based AIMD simulations has been proposed as a solution.[94,117,118] Embracing computational models that have the performance in between the DFT and RFF can be an elective choice. The widely tested method for QMMD simulations of the condensed phase system is the density functional tight-binding (DFTB) method,[119–121] which is derived from DFT with careful approximations. The DFTB method satisfies both accuracy and efficiency with elaborated parameterizations. Previous studies have reported the imperfect water interactions in the bulk condition,[122–126] theoretical extensions for the improved description of the H-bond,[110,111,127–134] and the specific parameter optimization,[113,135,136] which may improve the performance of the DFTB method for conducting extensive sampling of PT events in aqueous solutions. To facilitate the large-scale BOMD simulations, the DFTB method may be combined with linear-scaling techniques such as the fragment molecular orbital method[137–139] and the divide-and-conquer (DC) method[140–145] or with some sparse algebraic schemes.[146,147]

The DC-type DFTB-based MD simulations have been lately applied to proton dynamics in bulk water for a system containing a large number of atoms.[112,113] An interesting observation for H_3O^+ diffusion is the consistent description of both vehicular and structural diffusion constants relative to experimental ones[112] (see Table 1 for overall diffusion constants defined as the sum of two terms) as opposed to the constants calculated by estimation from smaller unit cell sizes.[123,125] This is likely a manifestation of the existence of an artifact in the small model system, namely the strengthened H-bond network introduced by the contributions from periodic images. In Reference 112, not only dynamical properties but also the proton diffusion barrier have agreed with the experimental values, exhibiting less than 0.5 kJ/mol error. Regarding OH^- diffusion, the DFTB potential fitted to structural properties at the Becke-Lee-Yang-Parr level has also resulted in qualitative production of dynamical and energetic properties.[113] Moreover, the simulation has confirmed the decrease of the proton diffusion barrier with respect to the less-coordinated solvation structures. This observation supports the widely accepted PT mechanism.[10,11,71,76–82] Moreover, these simulation results indicate the importance of treating large and realistic systems. A larger system is beneficial to minimize unphysical mirror image interactions. In addition, it was shown that adopting a large system size will reduce the temperature fluctuations during the equilibration and production run.[112]

3 | PROTON TRANSFER IN ICE PHASES

The application of AIMD to the PT process in ice, either crystalline or amorphous forms of water,[148,149] can be straightforwardly motivated once its reasonable performance has been achieved in bulk water. In such solid systems, the presence of an excess proton or a proton hole is represented as an ionic defect, which becomes the origin of pure structural diffusion under the condition that the oxygen atom positions rarely changes. For example, experimental measurements have shown proton diffusivity in an ordinary hexagonal (ice I_h) or metastable cubic (ice I_c) form of ice approximately 10 times faster than that in the liquid phase at the same temperature.[64,150–156] Despite several explanations have been proposed,[157–163] the investigation of the anomalously fast PT event in the ice phases remains an active research field.

Similar to the case of bulk water, the description of H-bond as accurate as possible in ice phases is critical. The static properties of various polymorph ice structures, including equilibrium crystal structure, binding energy, and bulk modulus, have been assessed for different levels of quantum chemical methods.[164–169] One crucial conclusion from the comparison among DFT functionals is that long-range dispersion correction benefits the improved performance.[164,166,168,169] Popular PBE functional was found to underestimate the sublimation energy of high-pressure ice by 15% compared to the experiment.[170] Sufficiently large basis sets ("*tier2*" for H and "*tier3*" for O) are required since it was shown to significantly affect the calculated lattice energies.[169] Perdew and coworkers[171] show that the meta-GGA functionals, namely revised Tao-Perdew-Staroverov-Scuseria and meta-generalized gradient approximation made simple (MGGA-MS) yield a better description on the sublimation energy and equilibrium volume of low-pressure phase of ice, even without employing the dispersion correction. The dispersion correction is necessary for the GGA functionals to improve their accuracy in describing these properties.[171] Despite the MGGA-MS underestimates the sublimation energy of high-pressure phases of ice, the dispersion correction was confirmed to improve the description for ambient-pressure phases of ice.[171] Moreover, the extensive benchmark has confirmed the adequate accuracy of dispersion-corrected DFTB for low-density phases.[168] These results support the application of AIMD to proton dynamics.

Beside the numerical assessments, a number of first-principles studies have been performed for the ice system in the scope of vibrational frequency analyses[172–182] and the PT phenomena.[183–186] As for the latter, Ohmine and co-workers have determined the potential energy surfaces of PT in proton-ordered/disordered ice structures using the QM/MM approach.[185] An important highlight is that the distances between oxygen atoms in the excess proton moiety are shortened by two types of forces—an attractive force due to the presence of the excess proton in the middle of two oxygen atoms (O─H^+─O) and a repulsive force from the fourth-coordinating water molecule on the protonated water molecule.[185] The existing local structure of water molecules around the H_3O^+ ion strictly differs from that of the liquid water, in which the term of Eigen or Zundel no longer exists. Due to the environment constraining the oxygen distances, the formation of the Zundel species is prevented. The absence of Zundel–Eigen interchange during the transfer leads to concerted PT events, which then enhance the PT rate.[185] Moreover, the Zundel form may exist in the liquid water due to the absence of the repulsive force from the fourth-coordinating water molecule.

For elucidating the relationship between the confined structure in ice phases and proton diffusivity, the BOMD simulations have been recently carried out for ice I_h and ice I_c with low density as well as two high-density structures (ice III and melted ice VI) at the DFTB level.[183] The averaged local bond order parameters,[187] which quantify the degree of cubic ($\langle q_4 \rangle$) and hexagonal ($\langle q_6 \rangle$) symmetries in the crystal structure, have been employed to extract the regularity of water molecule configuration. Figure 1 shows the correlation between $\langle q_4 \rangle$ and $\langle q_6 \rangle$ values, in which the clustered points clearly distinguish the different ice crystal structures. Importantly, the low- and high-density variants are distinguishable by hexagonality. The calculated structural diffusion constants at several temperatures are summarized in Table 2. The proton diffusivity in ice I_h and ice I_c is found to be faster than that in ice III and melted ice VI. The evaluation of structural and dynamical properties indicates that a higher hexagonal symmetry inducing delocalization of a positive charge is likely to be an essential factor for the fast PT event. In addition, the estimated proton diffusion barrier was only 0.5 kJ/mol higher than the experimental value, establishing the validity of DFTB simulations.[183,188]

On the other side of theoretical analysis using relatively low quantum chemical methods, the calibration of low-temperature AIMD simulations by nuclear quantum effects has been examined.[157,159,160] The recent study by Drechsel-Grau and Marx has demonstrated collective proton tunneling in a six-membered ring structure of ice I_h, which is schematically represented in Figure 2.[160] According to the AIMD approach combined with the path integral technique,[189–191] the first PT of $H^{(1)}$ to the adjacent oxygen atom $O^{(2)}$ is observed followed by the concerted movements of five other protons $H^{(2)}$–$H^{(6)}$. The energy barrier for the collective PT event is independent of the local structure in terms of the free energy profile (Figure 3) and the similarity of the calculated properties along the PT coordinates between chair and boat conformations.[160] Note that neither many-

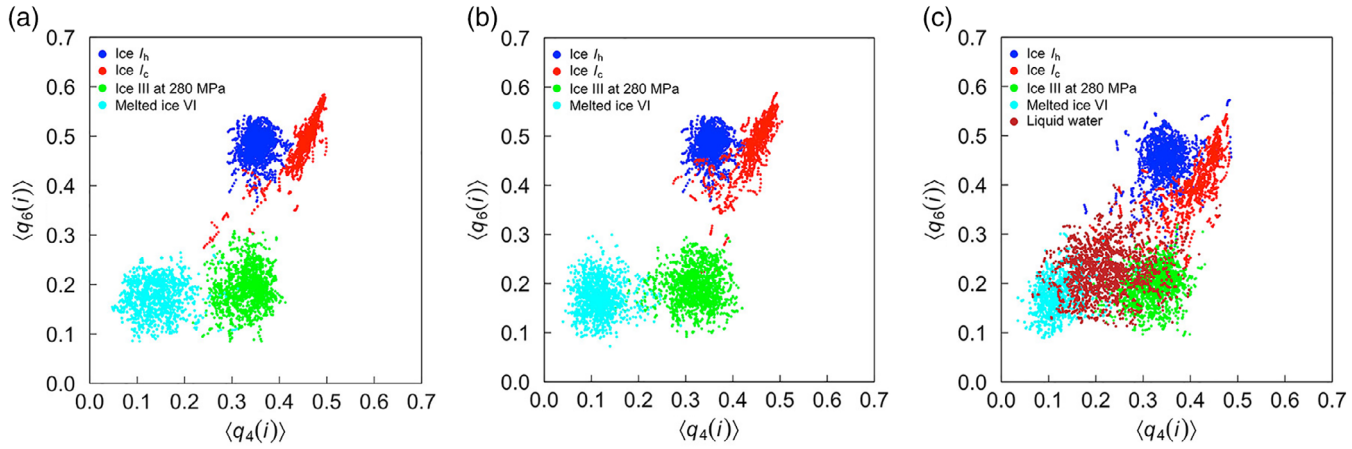

FIGURE 1 Correlation between the cubic ($\langle q_4(i)\rangle$) and hexagonal ($\langle q_6(i)\rangle$) symmetries for ice structures and liquid water estimated at (a) 230, (b) 250, and (c) 270 K. (Reprinted with permission from Reference 183. Copyright 2018 American Chemical Society)

TABLE 2 Estimated structural diffusion constants (in Å^2/ps) for ice structures based on MD simulations at the DFTB level. (Reprinted with permission from Reference 183. Copyright 2018 American Chemical Society)

T (K)	Ice I_h	Ice I_c	Ice III	Melted ice VI
50	0.10	0.00		
70	0.36	0.32		
120	0.94	0.72		
230	1.84	2.04	0.25	0.36
250	1.98	1.14	0.48	1.00
270	1.90	2.28	0.54	1.21

body proton tunneling nor multiple PT processes have been achieved at temperatures less than 100 K in the aforementioned DFTB simulations.[178]

In addition to the fundamental aspects of the PT process in the ice phase, recent AIMD studies successfully address other related issues such as chemical reactions on top of the ice surface,[192–195] ionization dynamics of the water dimer on the ice surface,[196–198] and ionization of acids on the quasi-liquid layer of ice.[199] Moreover, the PT event under the presence of an electric field has been investigated, in which the enhanced coupling between dipole moments and internal electric field leads to a faster diffusion in a more ferroelectric phase than that in ice I_h.[200] Elucidation of the PT process in ice from manifold theoretical viewpoints will enrich the information about H-bond systems.

4 | PROTON TRANSFER IN CONFINED WATER ENVIRONMENT

A confined water environment is a specific system created by the surrounding material in which water molecules are placed in a nanometer-sized vessel. The confined water is found in many materials including cells,[201–203] macromolecules,[204–206] supramolecule structures,[207,208] and gels.[209–212] Such a confined environment may lead to the phase transformation that is not present in the bulk condition under the same thermodynamical condition.[213–215] Moreover, the confined environment causes both slow and fast dynamics of water molecules, thus garnering significant attention from many research disciplines.[216,217] The slow dynamics of water in the region close to the hydrophilic chains of protein has been comprehensively reviewed by Bagchi[218] and theoretical research on MD simulations performed for water at the protein–solvent interface has been conducted.[219] It is noteworthy that the confinement results change with several properties, such as highly anisotropic orientational dynamics in carbon nanostructures,[220] dipole orientation in a narrow nanotube,[221] and liquid–liquid transition.[222]

The PT process in the confined water environment is one of the fascinating topics in AIMD. For example, Dellago et al. have reported fast proton mobility in a carbon nanotube (CNT) via both AIMD and RFF simulations.[223] The reported proton diffusion constant of 17 Å^2/ps is 18.1 times higher than the experimentally estimated diffusion constant.[224] Another AIMD

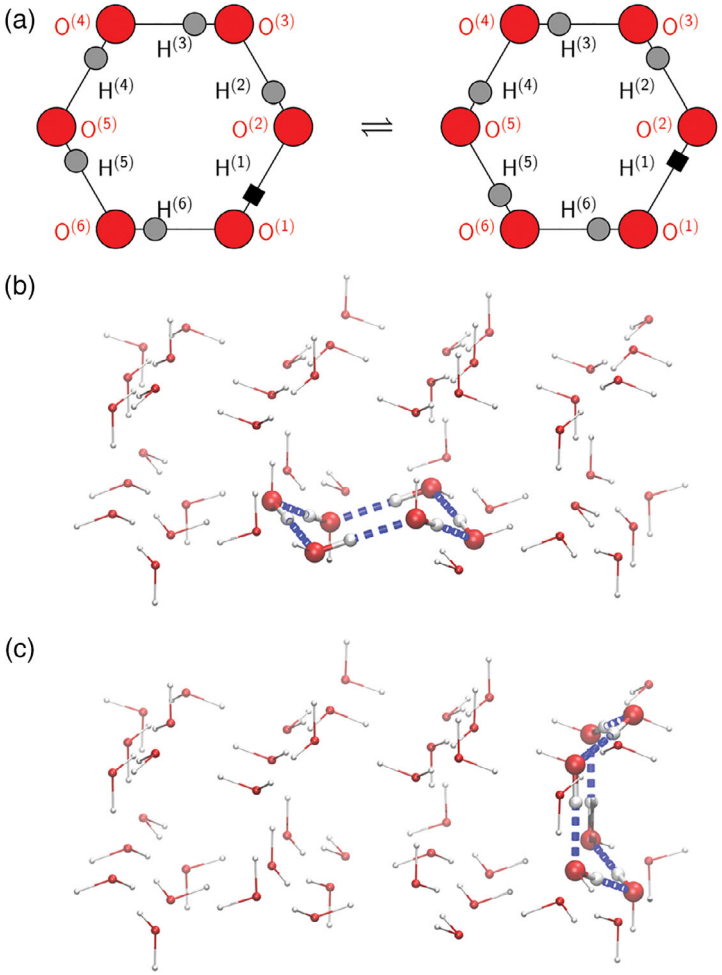

FIGURE 2 (a) Schematic representation of collective PT events in a six-membered ring of ice I_h structure. Red and gray circles represent the oxygen and hydrogen atoms, respectively, whereas the black square represents the deuteron in the case of the partially deuterated systems. The numbers in parentheses describe the label of the H-bonds. (b) and (c) display the chair and boat conformations existing in the proton-ordered ice I_h structure. (Reprinted with permission from Reference 160. Copyright 2017 Royal Society of Chemistry)

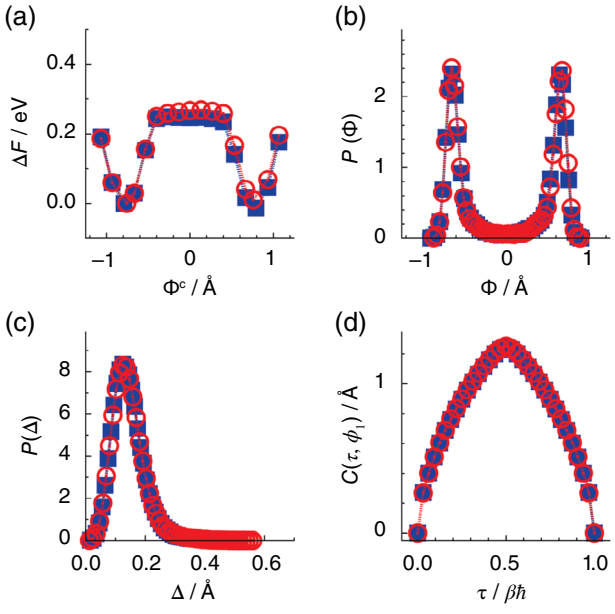

FIGURE 3 Comparison of the collective PT in chair (filled blue squares) and boat (empty red circles) conformations of the proton-ordered six-membered ring structure. (a) Free energy profile along the constraint PT coordinate, (b) probability distribution of the collective PT coordinate defined as $\phi = \sum_{i=1}^{6} \phi_i/6$, where $\phi_i = d(O^{(i)}H^{(i)}) - d(H^{(i)}O^{(i+1)})$ in a six-membered ring, (c) probability distribution of $\Delta = \left(\sum_{i=1}^{6} |\phi(\gamma,s) - \phi_i(\gamma,s)|^2/6\right)^{1/2}$, and (d) imaginary time correlation function $C(\tau,\phi_1) = \langle|\phi_1(\tau) - \phi_1(0)|^2\rangle^{1/2}$. (Reprinted with permission from Reference 160. Copyright 2017 Royal Society of Chemistry)

simulation has been performed to investigate the effect of the diameter and fluorination of the inner wall of CNT on the PT behavior.[225] The upper panel of Figure 4 shows the amount of H-bond formation between fluorine atoms and water molecules as a function of simulation time. The observed peaks clearly indicate that the smaller diameter particles prefer a greater

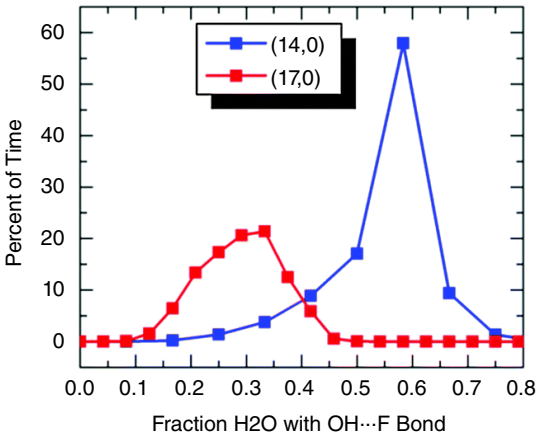

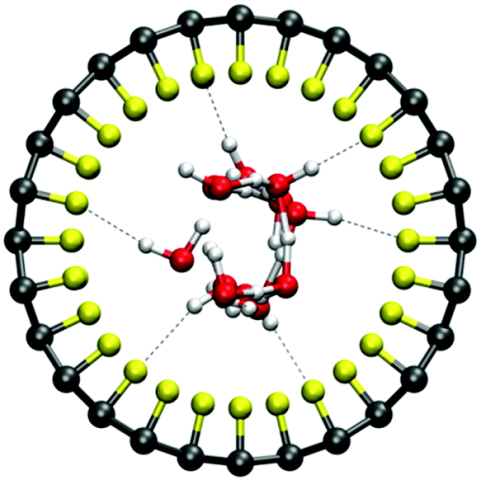

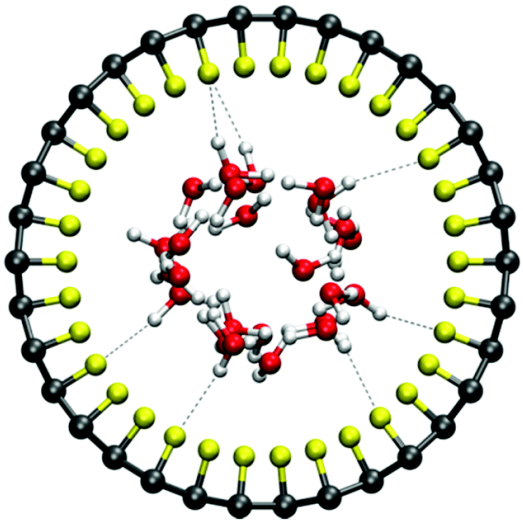

FIGURE 4 Water molecule configurations in the presence of an excess proton in two different fluorinated carbon nanotube (CNT) sizes, namely, 13.3 Å (bottom) and 11.0 Å (middle). The CNT with a larger and smaller diameter exhibits (14,0) and (17,0) chirality, respectively. Percent of time throughout the trajectory OH· · ·F H-bonds exist with respect to the fraction of interacting water molecules is also shown (top). (Reprinted with permission from Reference 224. Copyright 2014 Royal Society of Chemistry)

H-bond formation, which has been confirmed by the typical snapshots in the bottom panel of Figure 4. In addition, a comparison with a system without an excess proton in the confined water environment exhibited the superior interaction of the charged endohedral water structure with the functionalized sidewall.

To establish a qualitative explanation of change in PT behavior due to the fluorination of CNT, probability distribution functions as a function of PT coordinates have been evaluated in Reference 224. In Figure 5, a local minimum at $\delta = 0$ indicates a metastable Zundel form, that is, the proton is located between two water molecules. The Zundel form has been slightly dominant only in the case of fluorinated CNT with a small diameter. On the other hand, for fluorinated CNT with a large diameter, the opposite Zundel versus Eigen ratio has been obtained. The overall simulation results have implied that the

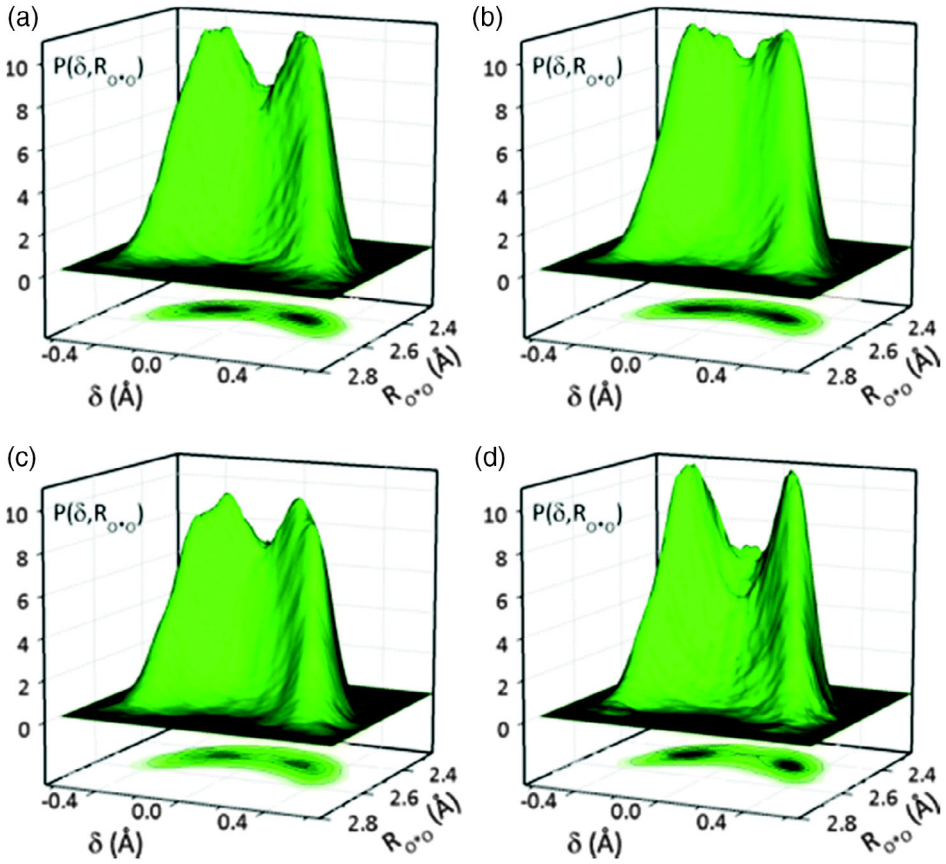

FIGURE 5 Probability distribution functions, $P(\delta,R_{O*O})$, of the PT coordinate defined as $\delta = R_{O*H^*} - R_{H*O}$ and the distance between the oxygen atoms, R_{O*O}, where "*" indicates the hydronium ion. Non-fluorinated carbon nanotubes (CNTs) with chirality (14,0) and (17,0) are shown in (a) and (b), respectively, whereas the fluorinated CNTs with chirality (14,0) and (17,0) are shown in (c) and (d), respectively. (Reprinted with permission from Reference 224. Copyright 2014 Royal Society of Chemistry)

stronger interaction of tightly confined water with fluorinated groups induces a directional PT process perpendicular to the tube axis. This explanation has been further supported by projection maps of the most active proton in the AIMD trajectories.[224]

Despite excluding many factors such as nuclear quantum effects, density of water, and distribution of fluorine atoms covering the inner channel, AIMD simulations have provided the valuable molecular mechanism and a possible way to further design the channel space with improved proton conduction performance. However, currently, the estimation of the diffusion constant or proton conductivity for systems more complex than pure water structures is considered to be a challenging task. This may be due to the difficulty of conducting sufficient statistical sampling in the limited system size. At least, it may be necessary to perform the production runs for tens of picoseconds, for example, longer than 20 or 100 ps for a large and small system sizes, respectively.[112,113,183] The simulations at the DFTB level may help to enhance the trajectory sampling as performed for the bulk liquid water and modeled channel.[112]

In spite of the computational cost issue, structural and dynamical properties of H_3O^+ and OH^- in CNT were successfully assessed at the DFT level.[225] The simulations revealed that each H_3O^+ or OH^- ion is two-coordinated to donate or accept a proton. Since no H-bond breaking is required, the PT rates become faster than the case of the bulk liquid water. It was also confirmed that the migration kinetics of OH^- is slightly faster than that of H_3O^+ ion, which is opposite to the nature of their diffusivity in the bulk liquid water. Another theoretical study reported that the local structure around the H_3O^+ ion is not significantly affected by the confinement. As a result, the dynamics of PT event is similar to that in the bulk phase,[226] which depends on the material that confines the ionic defect. Note that for the latter case, the confinement was created by incorporating water in the mackinawite sheets FeS mineral.[226,227]

In contrast to the case of bulk liquid water and ice systems, the simulations of PT in confined water system can be performed using at the PBE level with ultrasoft pseudopotentials, without the dispersion correction.[226] Adding the dispersion correction may deteriorate the system containing H-bond network. Such evidence may limit the applicability of the dispersion-corrected functional on the system containing a more complex material than the bulk liquid water system. Since the plane wave basis is usually employed, the size of basis set is defined by its cutoff, namely, 25 Ry (~340 eV)[226] and 400 eV.[224]

5 | PROTON TRANSFER IN CARBON DIOXIDE CAPTURE AND STORAGE MATERIALS

Carbon dioxide capture and storage (CCS) is one of the industrial technologies aimed at solving the problem of excess CO_2 present in the atmosphere.[228–231] To urgently resolve such an environmental issue, the practical use of CO_2 chemical absorption and regeneration processes is of paramount importance. While novel absorbents have been developed,[232–236] there has been an increasing interest in developing a rational material design scheme on the basis of the elementary reactions of CO_2 capture in order to further enhance the process performance. The computational studies have made a significant impact on the understanding of the mechanism and the evaluation of the microscopic properties, as observed in the recent comprehensive reviews.[237–239] In this section, we highlight the success of AIMD simulations in exploring the dynamic process of CO_2 absorption in which PT is an inseparable event.

Among the CO_2 chemical absorbents, aqueous amine solution is the most widely used.[240] The application of AIMD to CO_2 absorption and regeneration processes has unveiled many mechanistic details that occur between CO_2 and amines, solvent water molecules, and water constituent ions.[241–257] The extensively investigated reaction is the formation of carbamate via a zwitterion intermediate,[241–247,249,251–255,257] possibly because it is experimentally difficult to probe the metastable chemical species. After the carbon atom of CO_2 approaches the nitrogen atom of amine molecules, the binding complex experiences deprotonation of the nitrogen atom by being attacked by a base with high proton affinity. The representative snapshots of CO_2 capture in a monoethanolamine solution obtained by Hwang and co-workers are shown in Figure 6, where the solvent water molecule serves as a base.[246] The PT event in Figure 6b proceeded rapidly because PT may be associated with the insignificant energy barrier of less than 0.1 eV, which is estimated from static quantum chemical calculations.[238] Note that other investigated elementary reactions in Figure 6c–e also involve the PT processes with structural diffusions or concerted migrations.

The recent large-scale DFTB-based MD simulations have investigated the participation of the OH^- ion in the zwitterion mechanism.[254] The explicit inclusion of OH^- in the system has led to the abstraction of the prevailing proton by the anion instead of the solvent water molecules. This observation arises from two factors: the stronger proton acceptor of negatively charged species and the increased probability of establishing a close contact with CO_2 in favor of the structural diffusivity of OH^-. Sakti et al.[254] have further estimated rate constants of the zwitterion formation reaction by fitting time-course changes of chemical species to the kinetic model. Their analysis showed a reaction rate of zwitterion deprotonation slower than that of formation; this may be interpreted as the importance of OH^- ion concentration for producing more CO_2 absorbed compound (carbamate ion).

The bicarbonate ion is another chemical product formed during the CO_2 capture process.[258,259] The AIMD simulations have not extensively targeted the bicarbonate formation reaction in an aqueous system.[250,256,258,260,261] Nakai et al.[250] have gained molecular insights from structural and electronic analyses that the Grotthuss-type diffusion of the OH^- ion plays the key role in CO_2 interaction. They have also observed various chemical reactions involving the PT process during the sampling of 100 trajectories and further illustrated the direct PT mechanism in the CO_2 regeneration process. The PT process can be considered to dominate the major part of the chemical absorption in CCS.

The theoretical estimation of acidity (pK_a) of the protonated amine serve as an important research area related to CCS.[233] The AIMD simulations[262–265] have contributed to compute pK_a values of acid molecules by considering the explicit solution environment and the temperature effect with the help of the metadynamics sampling technique.[266–268] Recently, the excellent performance of the DFTB-based metadynamics approach has been verified for the calculation of pK_a values of amines.[269] The comparison with more than 30 experimental data[270–273] has resulted in the mean absolute deviation of 0.09 pK_a units (Table 3) and correlation coefficient of 0.990. By using the established protocol, new candidates for the CO_2 absorption process can be explored.

6 | CONCLUSION

Recent theoretical studies on PT in various water environments have highlighted the importance of the theoretical development for describing the water systems. Despite some theoretical issues and limitations, qualitative and quantitative properties associated with the PT process have been successfully evaluated and are found to be comparable with the experimental evidence. Along with more developed theoretical methods, the reason for OH^- diffusion to be slower than that of H_3O^+ in bulk liquid water has been revealed[100] and complemented the pre-solvation scenarios explained by AIMD simulations at the GGAs and DFTB levels.[10,112,113] While the accuracy of the DFT-based MD simulations depend on the choice of functional and the size of basis set, the DFTB methods relies on the performance of the parameter set. As previously examined by Choi et al.,[129]

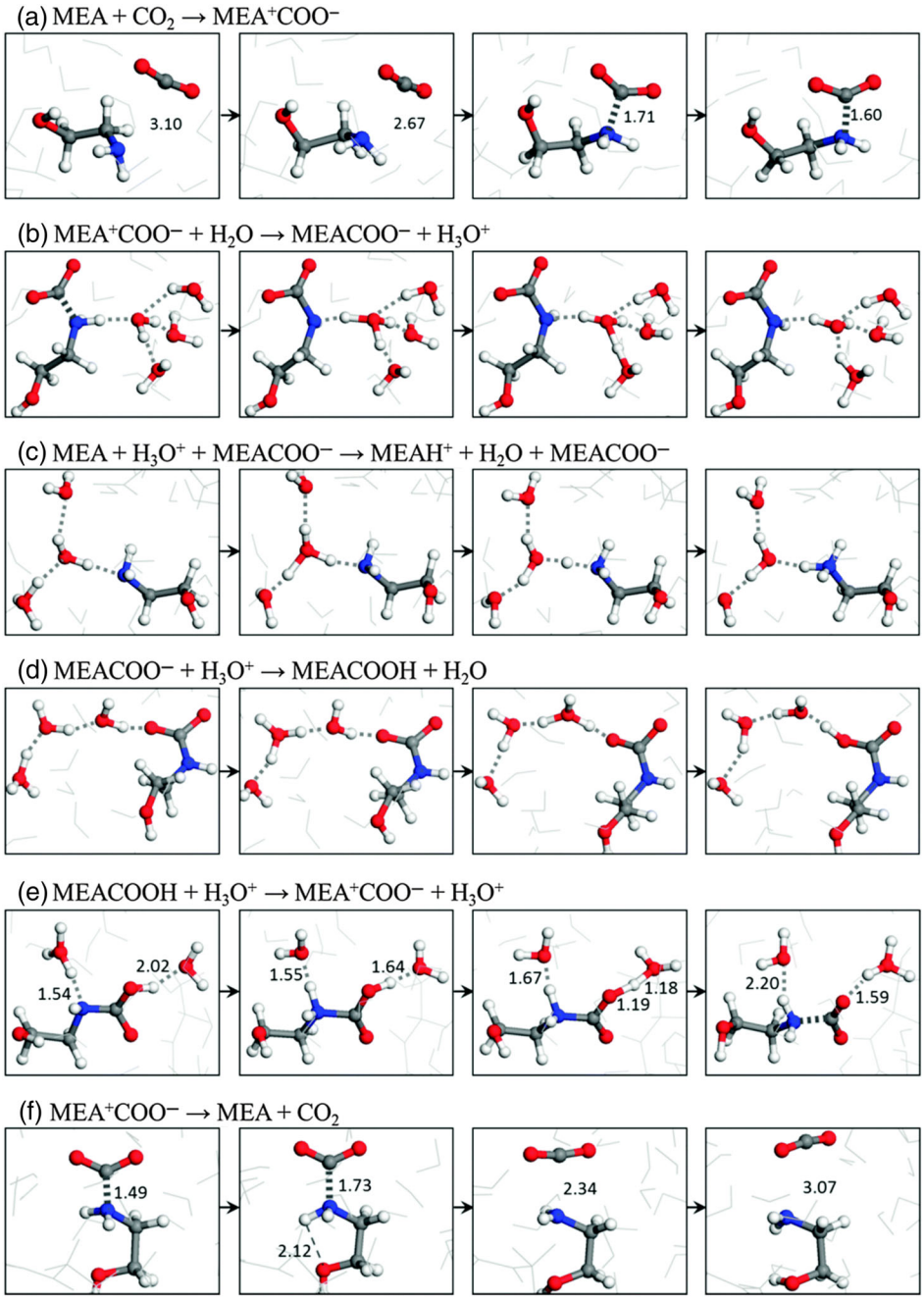

FIGURE 6 Snapshots of the ab initio molecular dynamics simulations describing the elementary reactions during the CO_2 absorption in an aqueous monoethanolamine solution. (Reprinted with permission from Reference 246. Copyright 2015 Royal Society of Chemistry)

the extension of the second-order to the third-order DFTB did not significantly improve the structure and dynamics of PT in liquid water. In fact, it was also found that the former one has better description of PT dynamics. Incorporating the diffusion correction in the MD simulation has not been confirmed to improve the structure and dynamics of H_3O^+ and OH^- ions in liquid water. Therefore, more thorough benchmark simulations at the DFTB level will be valuable assets for further improvement on the computational methodology.

At a low-temperature regime, in spite of high translational and rotational barriers that prevent vehicular diffusion, proton diffusivity is not negligible. The computer simulations have provided a theoretical evidence of faster diffusivity in the ice phase than that in bulk liquid water,[176] though occasionally the PT process is suppressed by the formation of a H_3O^+ ion with long shelf life. Moreover, fast proton diffusivity can be observed in a confined water environment created inside the nanochannel or porous materials. In such a confined water structure, once a charge defect is created, the proton diffusivity can be accelerated up to 18 times faster than that in liquid water.[221] H_3O^+ ion formation and water mobility are likely to be controlled by temperature, chemical environment related to hydrophobicity, and size of the nanoporous materials.[222] Furthermore, the PT process is essential in the chemical absorption and regeneration processes of the CCS technology. The in-depth

TABLE 3 Experimental and estimated pK_a values calculated from density functional tight-binding-based metadynamics simulations[269]

Entry	Amine	Abbreviation	pK_a (Calculated)	pK_a (Experimental)
1	1-Piperidinepropanolamine	1-PPP	9.32	9.43[a]
2	2-(2-Aminoethoxy)ethanol	2-AEE	9.49	9.42[b]
3	2-(Diisopropylamino)ethanol	2-DIPA	9.27	9.11[c]
4	2-Piperidineethanol	2-PPE	11.08	10.90[a]
5	2-Piperidinemethanol	2-PPM	10.47	10.60[a]
6	3-Dimethylamino-1-propanol	3-DMAP	9.30	9.27[a]
7	3-Morpholinopropylamine	3-MOPA	9.89	9.95[d]
8	3-Piperidinemethanol	3-PPM	10.98	10.80[a]
9	3-Piperidino-1,2-propanediol	3-PPPD	8.79	8.91[a]
10	3-Quinoclidinol	3-QCD	10.22	10.10[a]
11	4,2-Hydroxyethylmorpholine	4,2-HEMO	6.82	6.90[d]
12	2-Amino-2-ethyl-1,3-propanediol	AEPD	8.78	8.82[b]
13	2-Amino-2-methyl-1-propanol	AMP	9.16	9.23[b]
14	Diethanolamine	DEA	8.80	8.88[a]
15	Diisopropanolamine	DIPA	8.80	8.88[a]
16	*N*,*N*-Dimethylisopropanolamine	DMIPA	9.45	9.47[d]
17	2-(Ethylamino)ethanol	EAE	10.00	10.00[a]
18	Ethyldiethanolamine	EDEA	8.66	8.80[d]
19	Methyldiethanolamine	MDEA	8.43	8.31[c]
20	Monoethanolamine	MEA	9.14	9.09[a]
21	Methylmonoethanolamine	MMEA	9.94	9.85[b]
22	3-Amino-1-propanol	MPA	9.86	9.96[b]
23	Piperazine	PZ	9.30	9.38[c]
24	Serinol(2-aminopropane-1,3-diol)	SAPD	8.58	8.55[a]
25	2-(*tert*-Butylamino)ethanol	TBAE	9.76	9.70[a]
26	Triethanolamine	TEA	7.41	7.45[b]
27	Tris(hydroxymethyl)aminomethane	THMAM	8.16	8.08[a]
28	Tris[2-(2-methoxyethoxy)ethyl]amine	TMEEA	6.67	6.69[a]
29	Tricine	TRC	8.00	8.10[a]
30	Triethylamine	TREA	10.30	10.32[b]
31	*n*-Cyclohexylethanolamine	*n*-CHEA	9.89	10.10[a]
32	*n*-Cyclopentylethanolamine	*n*-CPEA	10.25	10.10[a]
33	*n*-Cyclopropylethanolamine	*n*-CPREA	8.50	8.40[a]
34	*tert*-Butyldiethanolamine	*t*-BDEA	8.92	9.03[d]
Mean absolute deviation			0.09	

[a]Reference 270.
[b]Reference 271.
[c]Reference 272.
[d]Reference 273.

understanding of the reaction mechanisms and calculation of the pK_a values as a useful factor affecting CO_2 absorption capability will boost future industrial applications of the PT process.

Classical MD simulations can hardly treat the PT event due to the inclusion of formation and cleavage of chemical bonds. On the other hand, recent QMMD simulations successfully rendered the mechanism, structure, dynamic, and energetic properties of the PT event, based on the careful treatments. First, the accuracy of the DFT method to describe the PT depends on the

choice of functionals[94] and the size of basis set.[118] One can tune the accuracy by adding the dispersion correction with many possible choice of dispersion models.[131,176] Similarly, the accuracy of the DFTB methods rely on their inbuilt parameter set. A good DFTB water models were developed to describe the structural[139] and dynamical properties via a specific parameterization scheme that limits the applicability for complex applications. A more general parameterization scheme is necessary for improving the transferability of parameters.[274] Second, frontier PT applications require a computational method that able to treat a large system size. Despite the QM/MM approach is one of sophisticated methods to tackle a big system, the ubiquitous nature of PT requires one to carefully choose the size of QM layer that can correctly capture the proton movements. A full QM treatment is arguably necessary for handling such ubiquitous nature of PT. With a support from a massive parallelization, one could develop linear-scaling DFT[119,275,276] and DFTB methods.[147] The latter is more practical owe to a double benefit from cost efficiency of the DFTB method assisted by the DC method in a massive parallel computation scheme.[143–147]

ACKNOWLEDGMENTS

The authors are grateful for the support by a Grant-in-Aid for Scientific Research (A) "KAKENHI JP26248009" from the Japan Society for the Promotion of Science (JSPS), a Grant-in-Aid for Challenging and Exploratory Research "KAKENHI 15K13629" from the Ministry of Education, Culture, Sports, Science, and Technology (MEXT), Japan, by MEXT as "Priority Issue on Post-K computer" (Development of new fundamental technologies for high-efficiency energy creation, conversion/storage, and use), and "Element Strategy Initiative for Catalysts and Batteries (ESICB)" project.

CONFLICT OF INTEREST

The authors have declared no conflicts of interest for this article.

ORCID

Aditya W. Sakti https://orcid.org/0000-0003-1515-4400
Hiromi Nakai https://orcid.org/0000-0001-5646-2931

REFERENCES

1. Kreuer K-D. Proton conductivity: Materials and applications. *Chem Mater*. 1996;*8*:610–641.
2. Decoursey TE. Voltage-gated proton channels and other proton transfer pathways. *Physiol Rev*. 2003;*83*:475–579.
3. Wraight CA. Chance and design—Proton transfer in water, channels and bioenergetic proteins. *Biochim Biophys Acta Bioenerg*. 2006;*1757*: 886–912.
4. Mulkidjanian AY, Heberle J, Cherepanov DA. Protons @ interfaces: Implications for biological energy conversion. *Biochim Biophys Acta Bioenerg*. 2006;*1757*:913–930.
5. Miyake T, Rolandi M. Grotthuss mechanisms: From proton transport in proton wires to bioprotonic devices. *J Phys Condens Matter*. 2016;*28*: 023001.
6. de Grotthius CJT. Memoir upon the decomposition of water, and of the bodies which it holds in solution, by means of galvanic electricity. *Philos Mag*. 1806;*25*:330–339.
7. Agmon N. The Grotthuss mechanism. *Chem Phys Lett*. 1995;*244*:456–462.
8. Cukierman S. Et tu, Grotthuss! And other unfinished stories. *Biochim Biophys Acta Bioenerg*. 2006;*1757*:876–885.
9. Marx D. Proton transfer 200 years after von Grotthuss: Insights from ab initio simulations. *Chemphyschem*. 2006;*7*:1848–1870.
10. Tuckerman ME, Chandra A, Marx D. Structure and dynamics of OH^- (aq). *Acc Chem Res*. 2006;*39*:151–158.
11. Marx D, Chandra A, Tuckerman ME. Aqueous basic solutions: Hydroxide solvation, structural diffusion, and comparison to the hydrated proton. *Chem Rev*. 2010;*110*:2174–2216.
12. Agmon N, Bakker HJ, Campen RK, et al. Protons and hydroxide ions in aqueous systems. *Chem Rev*. 2016;*116*:7642–7672.
13. Tersoff J. New empirical approach for the structure and energy of covalent systems. *Phys Rev B*. 1988;*37*:6991–7000.
14. Stuart SJ, Tutein AB, Harrison JA. A reactive potential for hydrocarbons with intermolecular interactions. *J Chem Phys*. 2000;*112*:6472–6486.
15. van Duin ACT, Dasgupta S, Lorant F, Goddard WA III. ReaxFF: A reactive force field for hydrocarbons. *J Phys Chem A*. 2001;*105*: 9396–9409.
16. Brenner DW, Shenderova OA, Harrison JA, Stuart SJ, Ni B, Sinnott SB. A second-generation reactive empirical bond order (REBO) potential energy expression for hydrocarbons. *J Phys Condens Matter*. 2002;*14*:783–802.
17. Senftle TP, Hong S, Islam MM, et al. The ReaxFF reactive force-field: Development, applications and future directions. *npj Comput Mater*. 2016;*2*:15011.

18. Mahadevan TS, Garofalini SH. Dissociative water potential for molecular dynamics simulations. *J Phys Chem B*. 2007;*111*:8919–8927.
19. Lee SH, Rasaiah JC. Proton transfer and the mobilities of the H^+ and OH^- ions from studies of a dissociating model for water. *J Chem Phys*. 2011;*135*:124505.
20. Pinilla C, Irani AH, Seriani N, Scandolo S. Ab initio parameterization of an all-atom polarizable and dissociable force field for water. *J Chem Phys*. 2012;*136*:114511.
21. Kale S, Herzfeld J, Dai S, Blank M. Lewis-inspired representation of dissociable water in clusters and Grotthuss chains. *J Biol Phys*. 2012;*38*: 49–59.
22. Lockwood GK, Garofalini SH. Lifetimes of excess protons in water using a dissociative water potential. *J Phys Chem B*. 2013;*117*: 4089–4097.
23. Zhang W, Chen X, van Duin ACT. Isotope effects in water: Differences of structure, dynamics, spectrum, and proton transport between heavy and light water from ReaxFF reactive force field simulations. *J Phys Chem Lett*. 2018;*9*:5445–5452.
24. Lentz J, Garofalini SH. Structural aspects of the topological model of the hydrogen bond in water on auto-dissociation via proton transfer. *Phys Chem Chem Phys*. 2018;*20*:16414–16427.
25. Warshel A, Weiss RM. An empirical valence bond approach for comparing reactions in solutions and in enzymes. *J Am Chem Soc*. 1980;*102*: 6218–6226.
26. Voth GA. Computer simulation of proton solvation and transport in aqueous and biomolecular systems. *Acc Chem Res*. 2006;*39*:143–150.
27. Knight C, Voth GA. The curious case of the hydrated proton. *Acc Chem Res*. 2012;*45*:101–109.
28. Vuilleumier R, Borgis D. Molecular dynamics of an excess proton in water using a non-additive valence bond force field. *J Mol Struct*. 1997; *436–437*:555–565.
29. Vuilleumier R, Borgis D. An extended empirical valence bond model for describing proton transfer in $H^+(H_2O)_n$ clusters and liquid water. *Chem Phys Lett*. 1998;*284*:71–77.
30. Vuilleumier R, Borgis D. Quantum dynamics of an excess proton in water using an extended empirical valence-bond Hamiltonian. *J Phys Chem B*. 1998;*102*:4261–4264.
31. Vuilleumier R, Borgis D. Transport and spectroscopy of the hydrated proton: A molecular dynamics study. *J Chem Phys*. 1999;*111*: 4251–4266.
32. Schmitt UW, Voth GA. Multistate empirical valence bond model for proton transport in water. *J Phys Chem B*. 1998;*102*:5547–5551.
33. Schmitt UW, Voth GA. The computer simulation of proton transport in water. *J Chem Phys*. 1999;*111*:9361–9381.
34. Day TJF, Soudackov AV, Čuma M, Schmitt UW, Voth GA. A second generation multistate empirical valence bond model for proton transport in aqueous systems. *J Chem Phys*. 2002;*117*:5839–5849.
35. Wu Y, Chen H, Wang F, Paesani F, Voth GA. An improved multistate empirical valence bond model for aqueous proton solvation and transport. *J Phys Chem B*. 2008;*112*:467–482.
36. Knight C, Maupin CM, Izvekov S, Voth GA. Defining condensed phase reactive force field from ab initio molecular dynamics simulations: The case of the hydrated excess proton. *J Chem Theory Comput*. 2010;*6*:3223–3232.
37. Chen H, Voth GA, Agmon N. Kinetics of proton migration in liquid water. *J Phys Chem B*. 2010;*114*:333–339.
38. Knight C, Lindberg GE, Voth GA. Multiscale reactive molecular dynamics. *J Chem Phys*. 2012;*137*:22A525.
39. Park K, Lin W, Paesani F. A refined MS-EVB model for proton transport in aqueous environments. *J Phys Chem B*. 2012;*116*:343–352.
40. Tahat A, Martí J. Dynamical aspects of intermolecular proton transfer in liquid water and low-density amorphous ices. *Phys Rev E*. 2014;*89*: 052130.
41. Tse Y-LS, Chen C, Lindberg GE, Kumar R, Voth GA. Propensity of hydrated excess protons and hydroxide anions for the air–water interface. *J Am Chem Soc*. 2015;*137*:12610–12616.
42. Biswas R, Carpenter W, Voth GA, Tokmakoff A. Molecular modeling and assignment of IR spectra of the hydrated excess proton in isotopically dilute water. *J Chem Phys*. 2016;*145*:154504.
43. Biswas R, Carpenter W, Fournier JA, Voth GA, Tokmakoff A. IR spectral assignments for the hydrated excess proton in liquid water. *J Chem Phys*. 2017;*146*:154507.
44. Biswas R, Voth GA. Role of solvation structure in the shuttling of the hydrated excess proton. *J Chem Sci*. 2017;*129*:1045–1051.
45. Chen C, Arntsen C, Voth GA. Development of reactive force fields using ab initio molecular dynamics simulation minimally biased to experimental data. *J Chem Phys*. 2017;*147*:161719.
46. Wick CD, Dang LX. Investigating hydroxide anion interfacial activity by classical and multistate empirical valence bond molecular dynamics simulations. *J Phys Chem A*. 2009;*113*:6356–6364.
47. Park K, Lin W, Paesani F. Fast and slow proton transfer in ice: The role of the quasi-liquid layer and hydrogen-bond network. *J Phys Chem B*. 2014;*118*:8081–8089.
48. Brewer ML, Schmitt UW, Voth GA. The formation and dynamics of proton wires in channel environments. *Biophys J*. 2001;*80*:1691–1702.
49. Cao Z, Peng Y, Yan T, Li S, Li A, Voth GA. Mechanism of fast proton transport along one-dimensional water chains confined in carbon nanotubes. *J Am Chem Soc*. 2010;*132*:11395–11397.
50. Tahat A, Martí J. Multistate empirical valence bond study of temperature and confinement effects on proton transfer in water inside hydrophobic nanochannels. *J Comput Chem*. 2016;*37*:1935–1946.
51. Wilhelm F, Schmickler W, Spohr E. Proton transfer to charged platinum electrodes. A molecular dynamics trajectory study. *J Phys Condens Matter*. 2010;*22*:175001.
52. Cao Z, Kumar R, Peng Y, Voth GA. Hydrated proton structure and diffusion at platinum surfaces. *J Phys Chem C*. 2015;*119*:14675–14682.

53. Tuckerman ME. Ab initio molecular dynamics: Basic concepts, current trends and novel applications. *J Phys Condens Matter*. 2002;*14*: R1297–R1355.
54. Kirchner B, di Dio PJ, Hutter J. Real-world predictions from ab initio molecular dynamics simulations. *Top Curr Chem*. 2012;*307*:109–154.
55. Hassanali AA, Cuny J, Verdolino V, Parrinello M. Aqueous solutions: State of the art in ab initio molecular dynamics. *Phil Trans R Soc A*. 2014;*372*:20120482.
56. Car R, Parrinello M. Unified approach for molecular dynamics and density-functional theory. *Phys Rev Lett*. 1985;*55*:2471–2474.
57. Hohenberg P, Kohn W. Inhomogeneous electron gas. *Phys Rev*. 1964;*136*:B864–B871.
58. Kohn W, Sham LJ. Self-consistent equations including exchange and correlation effects. *Phys Rev*. 1965;*140*:A1133–A1138.
59. Kohn W. Nobel lecture: Electronic structure of matter—Wave functions and density functionals. *Rev Mod Phys*. 1999;*71*:1253–1266.
60. Tuckerman ME, Laasonen K, Sprik M, Parrinello M. Ab initio simulations of water and water ions. *J Phys Condens Matter*. 1994;*6*: A93–A100.
61. Tuckerman M, Laasonen K, Sprik M, Parrinello M. Ab initio molecular dynamics simulation of the solvation and transport of H_3O^+ and OH^- ions in water. *J Phys Chem*. 1995;*99*:5749–5752.
62. Tuckerman M, Laasonen K, Sprik M, Parrinello M. Ab initio molecular dynamics simulation of the solvation and transport of hydronium and hydroxyl ions in water. *J Chem Phys*. 1995;*103*:150–161.
63. Zundel G, Metzger H. Energiebänder der tunnelnden Überschuß-Protonen in flüssigen Säuren. Eine IR-spektroskopische Untersuchung der Natur der Gruppierungen $H_5O_2^+$. *Z Phys Chem*. 1968;*58*:225–245.
64. Eigen M. Proton transfer, acid-base catalysis, and enzymatic hydrolysis. Part I: Elementary processes. *Angew Chem Int Ed*. 1964;*3*:1–19.
65. Berkelbach TC, Lee H-S, Tuckerman ME. Concerted hydrogen-bond dynamics in the transport mechanism of the hydrated proton: A first-principles molecular dynamics study. *Phys Rev Lett*. 2009;*103*:238302.
66. Baer M, Marx D, Mathias G. Theoretical messenger spectroscopy of microsolvated hydronium and Zundel cations. *Angew Chem Int Ed*. 2010; *49*:7346–7349.
67. Tse Y-LS, Knight C, Voth GA. An analysis of hydrated proton diffusion in ab initio molecular dynamics. *J Chem Phys*. 2015;*142*:014104.
68. Marx D, Tuckerman ME, Hutter J, Parrinello M. The nature of the hydrated excess proton in water. *Nature*. 1999;*397*:601–604.
69. Izvekov S, Voth GA. Ab initio molecular-dynamics simulation of aqueous proton solvation and transport revisited. *J Chem Phys*. 2005;*123*: 044505.
70. Markovitch O, Chen H, Izvekov S, Paesani F, Voth GA, Agmon N. Special pair dance and partner selection: Elementary steps in proton transport in liquid water. *J Phys Chem B*. 2008;*112*:9456–9466.
71. Chandra A, Tuckerman ME, Marx D. Connecting solvation shell structure to proton transport kinetics in hydrogen-bonded networks via population correlation functions. *Phys Rev Lett*. 2007;*99*:145901.
72. Swanson JMJ, Simons J. Role of charge transfer in the structure and dynamics of the hydrated proton. *J Phys Chem B*. 2009;*113*:5149–5161.
73. Tuckerman ME, Chandra A, Marx D. A statistical mechanical theory of proton transport kinetics in hydrogen-bonded networks based on population correlation functions with applications to acids and bases. *J Chem Phys*. 2010;*133*:124108.
74. Hassanali A, Prakash MK, Eshet H, Parrinello M. On the recombination of hydronium and hydroxide ions in water. *Proc Natl Acad Sci U S A*. 2011;*108*:20410–20415.
75. Hassanali A, Giberti F, Cuny J, Kühne TD, Parrinello M. Proton transfer through the water gossamer. *Proc Natl Acad Sci U S A*. 2013;*110*: 13723–13728.
76. Tuckerman ME, Marx D, Parrinello M. The nature and transport mechanism of hydrated hydroxide ions in aqueous solution. *Nature*. 2002; *417*:925–929.
77. Zhu Z, Tuckerman ME. Ab initio molecular dynamics investigation of the concentration dependence of charged defect transport in basic solutions via calculation of the infrared spectrum. *J Phys Chem B*. 2002;*106*:8009–8018.
78. Chen B, Ivanov I, Park JM, Parrinello M, Klein ML. Solvation structure and mobility mechanism of OH^-: A Car-Parrinello molecular dynamics investigation of alkaline solutions. *J Phys Chem B*. 2002;*106*:12006–12016.
79. Vassilev P, Louwerse MJ, Baerends EJ. Hydroxyl radical and hydroxide ion in liquid water: A comparative electron density functional theory study. *J Phys Chem B*. 2005;*109*:23605–23610.
80. Megyes T, Bálint S, Grósz T, Radnai T, Bakó I, Sipos P. The structure of aqueous sodium hydroxide solutions: A combined solution X-ray diffraction and simulation study. *J Chem Phys*. 2008;*128*:044501.
81. Chen B, Park JM, Ivanov I, Tabacchi G, Klein ML, Parrinello M. First-principles study of aqueous hydroxide solutions. *J Am Chem Soc*. 2002;*124*:8534–8535.
82. Renault JP, Vuilleumier R, Pommeret S. Hydrated electron production by reaction of hydrogen atoms with hydroxide ions: A first-principles molecular dynamics study. *J Phys Chem A*. 2008;*112*:7027–7034.
83. Agmon N. Mechanism of hydroxide mobility. *Chem Phys Lett*. 2000;*319*:247–252.
84. Asthagiri D, Pratt LR, Kress JD, Gomez MA. The hydration state of HO^- (aq). *Chem Phys Lett*. 2003;*380*:530–535.
85. Asthagiri D, Pratt LR, Kress JD, Gomez MA. Hydration and mobility of HO^- (aq). *Proc Natl Acad Sci U S A*. 2004;*101*:7229–7233.
86. Pavese M, Chawla S, Lu D, Lobaugh J, Voth GA. Quantum effects and the excess proton in water. *J Chem Phys*. 1997;*107*:7428–7432.
87. Marx D, Tuckerman ME, Parrinello M. Solvated excess protons in water: Quantum effects on the hydration structure. *J Phys Condens Matter*. 2000;*12*:A153–A159.
88. Li X-Z, Walker B, Michaelides A. Quantum nature of the hydrogen bond. *Proc Natl Acad Sci U S A*. 2011;*108*:6369–6373.

89. Giberti F, Hassanali AA, Ceriotti M, Parrinello M. The role of quantum effects on structural and electronic fluctuations in neat and charged water. *J Phys Chem B*. 2014;*118*:13226–13235.
90. Ceriotti M, Fang W, Kusalik PG, et al. Nuclear quantum effects in water and aqueous systems: Experiment, theory, and current challenges. *Chem Rev*. 2016;*116*:7529–7550.
91. Gillan MJ, Alfè D, Michaelides A. Perspective: How good is DFT for water? *J Chem Phys*. 2016;*144*:130901.
92. Morawietz T, Singraber A, Dellago C, Behler J. How van der Waals interactions determine the unique properties of water. *Proc Natl Acad Sci U S A*. 2016;*113*:8368–8373.
93. Ambrosio F, Miceli G, Pasquarello A. Structural, dynamical, and electronic properties of liquid water: A hybrid functional study. *J Phys Chem B*. 2016;*120*:7456–7470.
94. Pestana LR, Mardirossian N, Head-Gordon M, Head-Gordon T. Ab initio molecular dynamics simulations of liquid water using high quality meta-GGA functionals. *Chem Sci*. 2017;*8*:3554–3565.
95. Chen M, Ko H-Y, Remsing RC, et al. Ab initio theory and modeling of water. *Proc Natl Acad Sci U S A*. 2017;*114*:10846–10851.
96. Wiktor J, Ambrosio F, Pasquarello A. Note: Assessment of the SCAN+rVV10 functional for the structure of liquid water. *J Chem Phys*. 2017;*147*:216101.
97. Liu J, He X, Zhang JZH, Qi L-W. Hydrogen-bond structure dynamics in bulk water: Insights from ab initio simulations with coupled cluster theory. *Chem Sci*. 2018;*9*:2065–2073.
98. Zheng L, Chen M, Sun Z, et al. Structural, electronic, and dynamical properties of liquid water by ab initio molecular dynamics based on SCAN functional within the canonical ensemble. *J Chem Phys*. 2018;*148*:164505.
99. Pestana LR, Marsalek O, Markland TE, Head-Gordon T. The quest for accurate liquid water properties from first principles. *J Phys Chem Lett*. 2018;*9*:5009–5016.
100. Chen M, Zheng L, Santra B, et al. Hydroxide diffuses slower than hydronium in water because its solvated structure inhibits correlated proton transfer. *Nat Chem*. 2018;*10*:413–419.
101. Perdew JP, Ernzerhof M, Burke K. Rationale for mixing exact exchange with density functional approximations. *J Chem Phys*. 1996;*105*:9982–9985.
102. Wu X, Selloni A, Car R. Order-N implementation of exact exchange in extended insulating systems. *Phys Rev B*. 2009;*79*:085102.
103. Tkatchenko A, Scheffler M. Accurate molecular Van Der Waals interactions from ground-state electron density and free-atom reference data. *Phys Rev Lett*. 2009;*102*:073005.
104. Gaiduk AP, Gygi F, Galli G. Density and compressibility of liquid water and ice from first-principles simulations with hybrid functionals. *J Phys Chem Lett*. 2015;*6*:2902–2908.
105. Miceli G, de Gironcoli S, Pasquarello A. Isobaric first-principles molecular dynamics of liquid water with nonlocal van der Waals interactions. *J Chem Phys*. 2015;*142*:034501.
106. Wang Y, Perdew JP. Correlation hole of the spin-polarized electron gas, with exact small-wave-vector and high-density scaling. *Phys Rev B*. 1991;*44*:13298–13307.
107. Becke AD. Density-functional exchange-energy approximation with correct asymptotic behavior. *Phys Rev A*. 1988;*38*:3098–3100.
108. Lee C, Yang W, Parr RG. Development of the Colle-Salvetti correlation-energy formula into a functional of the electron density. *Phys Rev B*. 1988;*37*:785–789.
109. Boese AD, Doltsinis NL, Handy NC, Sprik M. New generalized gradient approximation functionals. *J Chem Phys*. 2000;*112*:1670–1678.
110. Elstner M. SCC-DFTB: What is the proper degree of self-consistency? *J Phys Chem A*. 2007;*111*:5614–5621.
111. Yang Y, Yu H, York D, Cui Q, Elstner M. Extension of the self-consistent-charge density-functional tight-binding method: Third-order expansion of the density functional theory total energy and introduction of a modified effective Coulomb interaction. *J Phys Chem A*. 2007;*111*:10861–10873.
112. Nakai H, Sakti AW, Nishimura Y. Divide-and-conquer-type density-functional tight-binding molecular dynamics simulations of proton diffusion in a bulk water system. *J Phys Chem B*. 2016;*120*:217–221.
113. Sakti AW, Nishimura Y, Nakai H. Divide-and-conquer-type density-functional tight-binding simulations of hydroxide ion diffusion in bulk water. *J Phys Chem B*. 2017;*121*:1362–1371.
114. Sluyters JH, Sluyters-Rehbach M. The mechanism of the hydrogen ion conduction in liquid light and heavy water derived from the temperature dependence of their limiting conductivies. *J Phys Chem B*. 2010;*114*:15582–15589.
115. Chen J, Michaelides A. Sticky when wet. *Nat Chem*. 2018;*10*:376–377.
116. Fischer SA, Dunlap BI, Gunlycke D. Correlated dynamics in aqueous proton diffusion. *Chem Sci*. 2018;*9*:7126–7132.
117. Lee H-S, Tuckerman ME. Structure of liquid water at ambient temperature from ab initio molecular dynamics performed in the complete basis set limit. *J Chem Phys*. 2006;*125*:154507.
118. Vandevondele J, Mohamed F, Krack M, Hutter J, Sprik M, Parrinello M. The influence of temperature and density functional models in ab initio molecular dynamics simulation of liquid water. *J Chem Phys*. 2005;*122*:014515.
119. Arita M, Bowler DR, Miyazaki T. Stable and efficient linear scaling first-principles molecular dynamics for 10000+ atoms. *J Chem Theory Comput*. 2014;*10*:5419–5425.
120. Osei-Kuffuor D, Fattebert J-L. A scalable O(N) algorithm for large-scale parallel first-principles molecular dynamics simulations. *Siam J Sci Comput*. 2014;*36*:C353–C375.

121. Fattebert J-L, Osei-Kuffuor D, Draeger EW, Ogitsu T, Krauss WD. Modeling dilute solutions using first-principles molecular dynamics: Computing more than a million atoms with over a million cores. *SC16: Proceedings of the International Conference for High Performance Computing, Networking, Storage and Analysis*. Piscataway, NJ: IEEE Press, 2016; p. 12–22.
122. Seifert G, Joswig J-O. Density-functional tight binding—An approximate density-functional theory method. *WIREs Comput Mol Sci*. 2012;*2*: 456–465.
123. Elstner M, Seifert G. Density functional tight binding. *Phil Trans R Soc A*. 2014;*372*:20120483.
124. Gaus M, Cui Q, Elstner M. Density functional tight binding: Application to organic and biological molecules. *WIREs Comput Mol Sci*. 2014; *4*:49–61.
125. Hu H, Lu Z, Elstner M, Hermans YW. Simulating water with the self-consistent-charge density functional tight binding method: From molecular clusters to the liquid state. *J Phys Chem A*. 2007;*111*:5685–5691.
126. Maupin CM, Aradi B, Voth GA. The self-consistent charge density functional tight binding method applied to liquid water and the hydrated excess proton: Benchmark simulations. *J Phys Chem B*. 2010;*114*:6922–6931.
127. Zheng G, Niklasson AMN, Karplus M. Lagrangian formulation with dissipation of Born–Oppenheimer molecular dynamics using the density-functional tight-binding method. *J Chem Phys*. 2011;*135*:044122.
128. Goyal P, Elstner M, Cui Q. Application of the SCC-DFTB method to neutral and protonated water clusters and bulk water. *J Phys Chem B*. 2011;*115*:6790–6805.
129. Choi TH, Liang R, Maupin CM, Voth GA. Application of the SCC-DFTB method to hydroxide water clusters and aqueous hydroxide solutions. *J Phys Chem B*. 2013;*117*:5165–5179.
130. Gaus M, Cui Q, Elstner M. DFTB3: Extension of the self-consistent-charge density-functional tight-binding method (SCC-DFTB). *J Chem Theory Comput*. 2011;*7*:931–948.
131. Řezáč J, Hobza P. Advanced corrections of hydrogen bonding and dispersion for semiempirical quantum mechanical methods. *J Chem Theory Comput*. 2012;*8*:141–151.
132. Domínguez A, Niehaus TA, Frauenheim T. Accurate hydrogen bond energies within the density functional tight binding method. *J Phys Chem A*. 2015;*119*:3535–3544.
133. Christensen AS, Elstner M, Cui Q. Improving intermolecular interactions in DFTB3 using extended polarization from chemical-potential equalization. *J Chem Phys*. 2015;*143*:084123.
134. Christensen AS, Kubař M, Cui Q, Elstner M. Semiempirical quantum mechanical methods for noncovalent interactions for chemical and biochemical applications. *Chem Rev*. 2016;*116*:5301–5337.
135. Řezáč J. Empirical self-consistent correction for the description of hydrogen bonds in DFTB3. *J Chem Theory Comput*. 2017;*13*:4804–4817.
136. Michoulier E, Amor NB, Rapacioli M, et al. Theoretical determination of adsorption and ionisation energies of polycyclic aromatic hydrocarbons on water ice. *Phys Chem Chem Phys*. 2018;*20*:11941–11953.
137. Simon A, Rapacioli M, Michoulier E, Zheng L, Korchagina K, Cuny J. Contribution of the density-functional-based tight-binding scheme to the description of water clusters: Methods, applications, and extension to bulk systems. *Mol Simul*. 2018;*45*:249–268. https://doi.org/10.1080/08927022.2018.1554903.
138. Doemer M, Liberatore E, Knaup JM, Tavernelli I, Rothlisberger U. In situ parameterisation of SCC-DFTB repulsive potentials by iterative Boltzmann inversion. *Mol Phys*. 2013;*111*:3595–3607.
139. Goyal P, Qian H-J, Irle S, et al. Molecular simulation of water and hydration effects in different environments: Challenges and developments for DFTB based models. *J Phys Chem B*. 2014;*118*:11007–11027.
140. Kitaura K, Ikeo E, Asada T, Nakano T, Uebayasi M. Fragment molecular orbital method: An approximate computational method for large molecules. *Chem Phys Lett*. 1999;*313*:701–706.
141. Nishimoto Y, Fedorov DG, Irle S. Density-functional tight-binding combined with the fragment molecular orbital method. *J Chem Theory Comput*. 2014;*10*:4801–4812.
142. Nishimoto Y, Nakata H, Fedorov DG, Irle S. Large-scale quantum-mechanical molecular dynamics simulations using density-functional tight-binding combined with the fragment molecular orbital method. *J Phys Chem Lett*. 2015;*6*:5034–5039.
143. Yang W, Lee T-S. A density-matrix divide-and-conquer approach for electronic structure calculations of large molecules. *J Chem Phys*. 1995; *103*:5674–5678.
144. Akama T, Kobayashi M, Nakai H. Implementation of divide-and-conquer method including Hartree-Fock exchange interaction. *J Comput Chem*. 2007;*28*:2003–2012.
145. Kobayashi M, Yoshikawa T, Nakai H. Divide-and-conquer self-consistent field calculation for open-shell systems: Implementation and application. *Chem Phys Lett*. 2010;*500*:172–177.
146. Kobayashi M, Nakai H. Divide-and-conquer approaches to quantum chemistry: Theory and implementation. In: Zalesny R, Papadopoulos MG, Mezey P, Leszczynski J, editors. *Linear-scaling techniques in computational chemistry and physics: Methods and applications*. Dordrecht: Springer, 2011; p. 97–127.
147. Nishizawa H, Nishimura Y, Kobayashi M, Irle S, Nakai H. Three pillars for achieving quantum mechanical molecular dynamics simulations of huge systems: Divide-and-conquer, density-functional tight-binding, and massively parallel computation. *J Comput Chem*. 2016;*37*: 1983–1992.
148. Nishimura Y, Nakai H. Parallel implementation of efficient charge–charge interaction evaluation scheme in periodic divide-and-conquer density-functional tight-binding calculations. *J Comput Chem*. 2018;*39*:105–116.

149. Scemama A, Renon N, Rapacioli M. A sparse self-consistent field algorithm and its parallel implementation: Application to density-functional-based tight binding. *J Chem Theory Comput*. 2014;*10*:2344–2354.
150. Keçeli M, Zhang H, Zapol P, Dixon DA, Wagner AF. Shift-and-invert parallel spectral transformation Eigensolver: Massively parallel performance for density-functional based tight-binding. *J Comput Chem*. 2016;*37*:448–459.
151. Bartels-Rausch T, Bergeron V, Cartwright JHE, et al. Ice structures, patterns, and processes: A view across the icefields. *Rev Mod Phys*. 2012;*84*:885–944.
152. Fuentes-Landete V, Mitterdorfer C, Handle PH, et al. Crystalline and amorphous ices. *Proceedings of the International School of Physics "Enrico Fermi"*. Amsterdam, Netherlands: IOS Press, 2015; p. 173–208.
153. Timmer RLA, Cox MJ, Bakker HJ. Direct observation of proton transfer in ice I_h using femtosecond spectroscopy. *J Phys Chem A*. 2010;*114*:2091–2101.
154. Uritski A, Presiado I, Erez Y, Gepshtein R, Huppert D. Temperature dependence of proton diffusion in I_h ice. *J Phys Chem C*. 2009;*113*:10285–10296.
155. Uritski A, Presiado I, Huppert D. Indication of a very large proton diffusion in ice I_h. *J Phys Chem C*. 2008;*112*:11991–12002.
156. Ayrton WE, Perry J. Ice as an electrolyte. *Proc Phys Soc London*. 1875;*2*:171–182.
157. Pines E, Huppert D. Geminate recombination proton-transfer reactions. *Chem Phys Lett*. 1986;*126*:88–91.
158. Pines E, Huppert D, Agmon N. Geminate recombination in excited-state proton-transfer reactions: Numerical solution of the Debye–Smoluchowski equation with backreaction and comparison with experimental results. *J Chem Phys*. 1988;*88*:5620–5630.
159. Bove LE, Klotz S, Paciaroni A, Sacchetti F. Anomalous proton dynamics in ice at low temperatures. *Phys Rev Lett*. 2009;*103*:165901.
160. Drechsel-Grau C, Marx D. Collective proton transfer in ordinary ice: Local environments, temperature dependence and deuteration effects. *Phys Chem Chem Phys*. 2017;*19*:2623–2635.
161. Drechsel-Grau C, Marx D. Tunnelling in chiral water clusters: Protons in concert. *Nat Phys*. 2015;*11*:216–218.
162. Drechsel-Grau C, Marx D. Quantum simulation of collective proton tunneling in hexagonal ice crystals. *Phys Rev Lett*. 2014;*112*:148302.
163. Benoit M, Marx D, Parrinello M. Tunnelling and zero-point motion in high-pressure ice. *Nature*. 1998;*392*:258–261.
164. Collier WB, Ritzhaupt G, Devlin JP. Spectroscopically evaluated rates and energies for proton transfer and Bjerrum defect migration in cubic ice. *J Phys Chem*. 1984;*88*:363–368.
165. Devlin JP. Vibrational spectra and point defect activities of icy solids and gas phase clusters. *Int Rev Phys Chem*. 1990;*9*:29–65.
166. Lee C-W, Lee P-R, Kim Y-K, Kang H. Mechanistic study of proton transfer and H/D exchange in ice films at low temperatures (100–140K). *J Chem Phys*. 2007;*127*:084701.
167. Hamada I. A van der Waals density functional study of ice I_h. *J Chem Phys*. 2010;*133*:214503.
168. Gillian MJ, Alfè D, Bygrave PJ, Taylor CR, Manby FR. Energy benchmarks for water clusters and ice structures from an embedded many-body expansion. *J Chem Phys*. 2013;*139*:114101.
169. Santra B, Klimeš J, Tkatchenko A, et al. On the accuracy of van der Waals inclusive density-functional theory exchange-correlation functionals for ice at ambient and high pressures. *J Chem Phys*. 2013;*139*:154702.
170. Santra B, Klimeš J, Alfè D, et al. Hydrogen bonds and van der Waals forces in ice at ambient and high pressures. *Phys Rev Lett*. 2011;*107*:185701.
171. Fang Y, Xiao B, Tao J, Sun J, Perdew JP. Ice phases under ambient and high pressure: Insights from density functional theory. *Phys Rev B*. 2013;*87*:214101.
172. Macher M, Klimeš J, Franchini C, Kresse G. The random phase approximation applied to ice. *J Chem Phys*. 2014;*140*:084502.
173. Kuo J-L, Klein ML, Kuhs WF. The effect of proton disorder on the structure of ice-Ih: A theoretical study. *J Chem Phys*. 2005;*123*:134505.
174. Li F, Skinner JL. Infrared and Raman line shapes for ice Ih. II. H_2O and D_2O. *J Chem Phys*. 2010;*133*:244504.
175. Li F, Skinner JL. Infrared and Raman line shapes for ice Ih. I. Dilute HOD in H_2O and D_2O. *J Chem Phys*. 2010;*132*:204505.
176. Murray ÉD, Galli G. Dispersion interactions and vibrational effects in ice as a function of pressure: A first principles study. *Phys Rev Lett*. 2012;*108*:105502.
177. Zhang J, Kuo J-L, Iitaka T. First principles molecular dynamics study of filled ice hydrogen hydrate. *J Chem Phys*. 2012;*137*:084505.
178. He X, Sode O, Xantheas SS, Hirata S. Second-order many-body perturbation study of ice Ih. *J Chem Phys*. 2012;*137*:204505.
179. Brandenburg JG, Maas T, Grimme S. Benchmarking DFT and semiempirical methods on structures and lattice energies for ten ice polymorphs. *J Chem Phys*. 2015;*142*:124104.
180. Liu Y, Ojamäe L. Raman and IR spectra of ice Ih and ice XI with an assessment of DFT methods. *J Phys Chem B*. 2016;*120*:11043–11051.
181. Gilliard P, Sode O, Hirata S. Second-order many-body perturbation study of ice Ih. *J Chem Phys*. 2014;*140*:174507.
182. Geiger P, Dellago C, Macher M, et al. Proton ordering of cubic ice Ic: Spectroscopy and computer simulations. *J Phys Chem C*. 2014;*118*:10989–10997.
183. Sakti AW, Nishimura Y, Chou C-P, Nakai H. Density-functional tight-binding molecular dynamics simulations of excess proton diffusion in ice I_h, ice I_c, ice III, and melted ice VI phases. *J Phys Chem A*. 2018;*122*:33–40.
184. Kobayashi C, Saito S, Ohmine I. Mechanism of proton transfer in ice. II. Hydration, modes, and transport. *J Chem Phys*. 2001;*115*:4742–4749.
185. Kobayashi C, Saito S, Ohmine I. Mechanism of fast proton transfer in ice: Potential energy surface and reaction coordinate analyses. *J Chem Phys*. 2000;*113*:9090–9100.
186. Drechsel-Grau C, Marx D. Exceptional isotopic-substitution effect: Breakdown of collective proton tunneling in hexagonal ice due to partial deuteration. *Angew Chem Int Ed*. 2014;*53*:10937–10940.

187. Lechner W, Dellago C. Accurate determination of crystal structures based on averaged local bond order parameters. *J Chem Phys*. 2008;*129*: 114707.
188. Presiado I, Lal J, Mamontov E, Kolesnikov AI, Huppert D. Fast proton hopping detection in ice I_h by quasi-elastic neutron scattering. *J Phys Chem C*. 2011;*115*:10245–10251.
189. Marx D, Parrinello M. Ab initio path-integral molecular dynamics. *Z Phys B*. 1994;*95*:143–144.
190. Marx D, Parrinello M. Ab initio path integral molecular dynamics: Basic ideas. *J Chem Phys*. 1996;*104*:4077–4082.
191. Marx D. Advanced Car–Parrinello techniques: Path integrals and nonadiabaticity in condensed matter simulations. *Lect Notes Phys*. 2006;*704*: 507–539.
192. Hirshberg B, Gerber RB. Formation of carbonic acid in impact of CO_2 on ice and water. *J Phys Chem Lett*. 2016;*7*:2905–2909.
193. Gerber RB, Varner ME, Hammerich AD, et al. Computational studies of atmospherically relevant chemical reactions in water clusters and on liquid water and ice surfaces. *Acc Chem Res*. 2015;*48*:399–406.
194. Shoaib MA, Choi CH. Adsorptions of formic and acetic acids on ice surface: Surface binding configurations and a possibility of interfacial proton transfer. *J Phys Chem C*. 2013;*117*:4181–4188.
195. Yoon Y, Shin S. Inter-layer proton transfer with a heterogeneous reaction on ice surface. *Chem Phys Lett*. 2008;*453*:45–48.
196. Tachikawa H. Ionization dynamics of water dimer on ice surface. *Surf Sci*. 2016;*647*:1–7.
197. Yoon Y, Shin S. Effects of surface trapped excess electrons on the dynamics of HCl adsorbed ice surfaces. *Chem Phys Lett*. 2007;*440*:83–86.
198. Brena B, Nordlund D, Odelius M, Ogasawara H, Nilsson A, Pettersson LGM. Ultrafast molecular dissociation of water in ice. *Phys Rev Lett*. 2004;*93*:148302.
199. Riikonen S, Parkkinen P, Halonen L, Gerber RB. Ionization of acids on the quasi-liquid layer of ice. *J Phys Chem A*. 2014;*118*:5029–5037.
200. Cassone G, Giaquinta PV, Saija F, Saitta AM. Proton conduction in water ices under an electric field. *J Phys Chem B*. 2014;*118*:4419–4424.
201. Disalvo EA, Lairion F, Martini F, et al. Structural and functional properties of hydration and confined water in membrane interfaces. *Biochim Biophys Acta Biomembr*. 2008;*1778*:2655–2670.
202. Bellissent-Funel M-C. Structure of confined water. *J Phys Condens Matter*. 2001;*13*:9165–9177.
203. England JL, Pande VS. Charge, hydrophobicity, and confined water: Putting past simulations into a simple theoretical framework. *Biochem Cell Biol*. 2010;*88*:359–369.
204. Chakraborty S, Kumar H, Dasgupta C, Maiti PK. Confined water: Structure, dynamics, and thermodynamics. *Acc Chem Res*. 2017;*50*: 2139–2146.
205. Floquet N, Coulomb JP, Dufau N, Andre G. Structure and dynamics of confined water in $AlPO_4$-5 zeolite. *J Phys Chem B*. 2004;*108*: 13107–13115.
206. Martin DR, Forsmo JE, Matyushov DV. Complex dynamics of water in protein confinement. *J Phys Chem B*. 2018;*122*:3418–3425.
207. Zanatta M, Girard A-L, Marin G, et al. Confined water in imidazolium based ionic liquids: A supramolecular guest@host complex case. *Phys Chem Chem Phys*. 2016;*18*:18297–18304.
208. Mallamace F, Earnshaw JC, Micali N, Trusso S, Vasi C. Dynamics of water confined in non-ionic amphiphiles supramolecular structures. *Physica A*. 1996;*231*:207–219.
209. Briman IM, Rébiscoul D, Diat O, Jollivet P, Zanotti J-M, Gin S. Dynamics of water confined in gel formed during glass alteration at a picosecond scale. *Procedia Earth Planet Sci*. 2013;*7*:733–737.
210. Fouzri A, Dorbez-Sridi R, Oumezzine M, Missaoui A. Water confined in silica gel at room temperature, X-ray diffraction study. *Int J Inorg Mater*. 2001;*3*:1315–1317.
211. Goracci G, Monasterio M, Jansson H, Cerveny S. Dynamics of nano-confined water in Portland cement—Comparison with synthetic C—S—H gel and other silicate materials. *Sci Rep*. 2017;*7*:8258.
212. Hou D, Zhao T, Ma H, Li Z. Reactive molecular simulation on water confined in the nanopores of the calcium silicate hydrate gel: Structure, reactivity, and mechanical properties. *J Phys Chem C*. 2015;*119*:1346–1358.
213. Bai J, Zeng XC. Polymorphism and polyamorphism in bilayer water confined to slit nanopore under high pressure. *Proc Natl Acad Sci U S A*. 2012;*109*:21240–21245.
214. Jinesh KB, Frenken JWM. Experimental evidence for ice formation at room temperature. *Phys Rev Lett*. 2008;*101*:036101.
215. Giovambattista N, Rossky PJ, Debenedetti PG. Effect of pressure on the phase behavior and structure of water confined between nanoscale hydrophobic and hydrophilic plates. *Phys Rev E*. 2006;*73*:041604.
216. Holt JK, Park HG, Wang Y, et al. Fast mass transport through sub-2-nanometer carbon nanotubes. *Science*. 2006;*312*:1034–1037.
217. Mukherjee B, Maiti PK, Dasgupta C, Sood AK. Jump reorientation of water molecules confined in narrow carbon nanotubes. *J Phys Chem B*. 2009;*113*:10322–10330.
218. Bagchi B. Water dynamics in the hydration layer around proteins and micelles. *Chem Rev*. 2005;*105*:3197–3219.
219. Bizzarri AR, Cannistraro S. Molecular dynamics of water at the protein−solvent interface. *J Phys Chem B*. 2002;*106*:6617–6633.
220. Mukherjee B, Maiti PK, Dasgupta C, Sood AK. Strongly anisotropic orientational relaxation of water molecules in narrow carbon nanotubes and nanorings. *ACS Nano*. 2008;*2*:1189–1196.
221. Mukherjee B, Maiti PK, Dasgupta C, Sood AK. Strong correlations and Fickian water diffusion in narrow carbon nanotubes. *J Chem Phys*. 2007;*126*:124704.
222. Koga K, Tanaka H, Zeng XC. First-order transition in confined water between high-density liquid and low-density amorphous phases. *Nature*. 2000;*408*:564–567.
223. Dellago C, Naor MM, Hummer G. Proton transport through water-filled carbon nanotubes. *Phys Rev Lett*. 2003;*90*:105902.

224. Ii JKC, Paddison SJ. Ab initio molecular dynamics simulations of water and an excess proton in water confined in carbon nanotubes. *Phys Chem Chem Phys*. 2014;*16*:17756–17769.
225. Bankura A, Chandra A. Hydroxide ion can move faster than an excess proton through one-dimensional water chains in hydrophobic narrow pores. *J Phys Chem B*. 2012;*116*:9744–9757.
226. Munoz-Santiburcio D, Wittekindt C, Marx D. Nanoconfinement effects on hydrated excess protons in layered materials. *Nat Commun*. 2013; *4*:2349.
227. Wittekindt C, Marx D. Water confined between sheets of Mackinawite FeS minerals. *J Chem Phys*. 2012;*137*:054710.
228. Haszeldine RS. Carbon capture and storage: How green can black be? *Science*. 2009;*325*:1647–1652.
229. D'Alessandro DM, Smit B, Long JR. Carbon dioxide capture: Prospects for new materials. *Angew Chem Int Ed*. 2010;*49*:6058–6082.
230. MacDowell N, Florin N, Buchard A, et al. An overview of CO_2 capture technologies. *Energ Environ Sci*. 2010;*3*:1645–1669.
231. Kenarsari SD, Yang D, Jiang G, et al. Review of recent advances in carbon dioxide separation and capture. *RSC Adv*. 2013;*3*:22739–22773.
232. Lee ZH, Lee KT, Bhatia S, Mohamed AR. Post-combustion carbon dioxide capture: Evolution towards utilization of nanomaterials. *Renew Sustain Energy Rev*. 2012;*16*:2599–2609.
233. Luis P, Van Gerven T, Van der Bruggen B. Recent developments in membrane-based technologies for CO_2 capture. *Prog Energy Combust Sci*. 2012;*38*:419–448.
234. Samanta A, Zhao A, Shimizu GKH, Sarkar P, Gupta R. Post-combustion CO_2 capture using solid sorbents: A review. *Ind Eng Chem Res*. 2012;*51*:1438–1463.
235. Dutcher B, Fan M, Russell AG. Amine-based CO_2 capture technology development from the beginning of 2013—A review. *ACS Appl Mater Interfaces*. 2015;*7*:2137–2148.
236. Heldebrant DJ, Koech PK, Glezakou V-A, Rousseau R, Malhotra D, Cantu DC. Water-lean solvents for post-combustion CO_2 capture: Fundamentals, uncertainties, opportunities, and outlook. *Chem Rev*. 2017;*117*:9594–9624.
237. Andreoni W, Pietrucci F. CO_2 capture in amine solutions: Modelling and simulations with non-empirical methods. *J Phys Condens Matter*. 2016;*28*:503003.
238. Yang X, Rees RJ, Conway W, Puxty G, Yang Q, Winkler DA. Computational modeling and simulation of CO_2 capture by aqueous amines. *Chem Rev*. 2017;*117*:9524–9593.
239. Stowe HM, Hwang GS. Fundamental understanding of CO_2 capture and regeneration in aqueous amines from first-principles studies: Recent progress and remaining challenges. *Ind Eng Chem Res*. 2017;*56*:6887–6899.
240. Rochelle GT. Amine scrubbing for CO_2 capture. *Science*. 2018;*325*:1652–1654.
241. Han B, Zhou C, Wu J, Tempel DJ, Cheng H. Understanding CO_2 capture mechanisms in aqueous monoethanolamine via first principles simulations. *J Phys Chem Lett*. 2011;*2*:522–526.
242. Guido CA, Pietrucci F, Gallet GA, Andreoni W. The fate of a zwitterion in water from ab initio molecular dynamics: monoethanolamine (MEA)-CO_2. *J Chem Theory Comput*. 2013;*9*:28–32.
243. Han B, Sun Y, Fan M, Cheng H. On the CO_2 capture in water-free monoethanolamine solution: An ab initio molecular dynamics study. *J Phys Chem B*. 2013;*117*:5971–5977.
244. Sumon KZ, Henni A, East ALL. Molecular dynamics simulations of proposed intermediates in the CO_2 + aqueous amine reaction. *J Phys Chem Lett*. 2014;*5*:1151–1156.
245. Ma C, Pietrucci F, Andreoni W. Capturing CO_2 in monoethanolamine (MEA) aqueous solutions: Fingerprints of carbamate formation assessed with first-principles simulations. *J Chem Theory Comput*. 2014;*5*(10):1672–1677.
246. Hwang GS, Stowe HM, Paek E, Manogaran D. Reaction mechanisms of aqueous monoethanolamine with carbon dioxide: A combined quantum chemical and molecular dynamics study. *Phys Chem Chem Phys*. 2015;*17*:831–839.
247. Ma C, Pietrucci F, Andreoni W. Capture and release of CO_2 in monoethanolamine aqueous solutions: New insights from first-principles reaction dynamics. *J Chem Theory Comput*. 2015;*11*:3189–3198.
248. Li H-C, Tsai M-K. A first-principle study of CO_2 binding by monoethanol amine and mono-n-propanolamine solutions. *Chem Phys*. 2015; *452*:9–16.
249. Stowe HM, Vilčiauskas L, Paek E, Hwang GS. On the origin of preferred bicarbonate production from carbon dioxide (CO_2) capture in aqueous 2-amino-2-methyl-1-propanol (AMP). *Phys Chem Chem Phys*. 2015;*17*:29184–29192.
250. Nakai H, Nishimura Y, Kaiho T, Kubota T, Sato H. Contrasting mechanisms for CO_2 absorption and regeneration processes in aqueous amine solutions: Insights from density-functional tight-binding molecular dynamics simulations. *Chem Phys Lett*. 2016;*647*:127–131.
251. Ma C, Pietrucci F, Andreoni W. Reaction dynamics of CO_2 in aqueous amines from ab initio molecular dynamics: 2-amino-2-methyl-1,-3-propanediol (AMPD) compared to monoethanolamine (MEA). *Theor Chem Acc*. 2016;*135*:60.
252. Stowe HM, Paek E, Hwang GS. First-principles assessment of CO_2 capture mechanisms in aqueous piperazine solution. *Phys Chem Chem Phys*. 2016;*18*:25296–25307.
253. Kubota Y, Ohnuma T, Bučko T. Carbon dioxide capture in 2-aminoethanol aqueous solution from ab initio molecular dynamics simulations. *J Chem Phys*. 2017;*146*:094303.
254. Sakti AW, Nishimura Y, Sato H, Nakai H. Divide-and-conquer density-functional tight-binding molecular dynamics study on the formation of carbamate ions during CO_2 chemical absorption in aqueous amine solution. *Bull Chem Soc Jpn*. 2017;*90*:1230–1235.
255. Lee B, Stowe HM, Lee KH, et al. Understanding CO_2 capture mechanisms in aqueous hydrazine via combined NMR and first-principles studies. *Phys Chem Chem Phys*. 2017;*19*:24067–24075.

256. Stowe HM, Hwang GS. Molecular insights into the enhanced rate of CO_2 absorption to produce bicarbonate in aqueous 2-amino-2-methyl-1-propanol. *Phys Chem Chem Phys*. 2017;*19*:32116–32124.
257. Kubota Y, Bučko T. Carbon dioxide capture in 2,2′-iminodiethanol aqueous solution from ab initio molecular dynamics simulations. *J Chem Phys*. 2018;*149*:224103.
258. Leung K, Nielsen IMB, Kurtz I. Ab initio molecular dynamics study of carbon dioxide and bicarbonate hydration and the nucleophilic attack of hydroxide on CO_2. *J Phys Chem B*. 2007;*111*:4453–4459.
259. Vaidya PD, Kenig EY. CO_2-alkanolamine reaction kinetics: A review of recent studies. *Chem Eng Technol*. 2007;*30*:1467–1474.
260. Stirling A, Pápai I. H_2CO_3 forms via HCO_3^- in water. *J Phys Chem B*. 2010;*114*:16854–16859.
261. Stirling A. HCO_3^- formation from CO_2 at high pH: Ab initio molecular dynamics study. *J Phys Chem B*. 2011;*115*:14683–14687.
262. Tummanapelli AK, Vasudevan S. Dissociation constants of weak acids from ab initio molecular dynamics using metadynamics: Influence of the inductive effect and hydrogen bonding on pK_a values. *J Phys Chem B*. 2014;*118*:13651–13657.
263. Tummanapelli AK, Vasudevan S. Ab initio molecular dynamics simulations of amino acids in aqueous solutions: Estimating pK_a values from metadynamics sampling. *J Phys Chem B*. 2015;*119*:12249–12255.
264. Tummanapelli AK, Vasudevan S. Estimating successive pK_a values of polyprotic acids from ab initio molecular dynamics using metadynamics: The dissociation of phthalic acid and its isomers. *Phys Chem Chem Phys*. 2015;*17*:6383–6388.
265. Tummanapelli AK, Vasudevan S. Ab initio MD simulations of the Brønsted acidity of glutathione in aqueous solutions: Predicting pK_a shifts of the cysteine residue. *J Phys Chem B*. 2015;*119*:15353–15358.
266. Laio A, Parrinello M. Escaping free-energy minima. *Proc Natl Acad Sci U S A*. 2002;*99*:12562–12566.
267. Ensing B, De Vivo M, Liu Z, Moore P, Klein ML. Metadynamics as a tool for exploring free energy landscapes of chemical reactions. *Acc Chem Res*. 2006;*39*:73–81.
268. Barducci A, Bonomi M, Parrinello M. Metadynamics. *WIREs Comput Mol Sci*. 2011;*1*:826–843.
269. Sakti AW, Nishimura Y, Nakai H. Rigorous pK_a estimation of amine species using density-functional tight-binding-based metadynamics simulations. *J Chem Theory Comput*. 2018;*14*:351–356.
270. Puxty G, Rowland R, Allport A, et al. Carbon dioxide postcombustion capture: A novel screening study of the carbon dioxide absorption performance of 76 amines. *Environ Sci Technol*. 2009;*43*:6427–6433.
271. Hamborg ES, Versteeg GF. Dissociation constants and thermodynamic properties of amines and alkanolamines from (293 to 393) K. *J Chem Eng Data*. 2009;*54*:1318–1328.
272. Tagiuri A, Mohamedali M, Henni A. Dissociation constant (pK_a) and thermodynamic properties of some tertiary and cyclic amines from (298 to 333) K. *J Chem Eng Data*. 2016;*61*:247–254.
273. Rayer AV, Sumon KZ, Jaffari L, Henni A. Dissociation constants (pK_a) of tertiary and cyclic amines: Structural and temperature dependences. *J Chem Eng Data*. 2014;*59*:3805–3813.
274. Chou C-P, Nishimura Y, Fan C-C, Mazur G, Irle S, Witek HA. Automatized parameterization of DFTB using particle swarm optimization. *J Chem Theory Comput*. 2016;*12*:53–64.
275. Gillan MJ, Bowler DR, Torralba AS, Miyazaki T. Order-N first-principles calculations with the conquest code. *Comput Phys Commun*. 2007;*177*:14–18.
276. Nakata A, Bowler DR, Miyazaki T. Optimized multi-site local orbitals in the large-scale DFT program CONQUEST. *Phys Chem Chem Phys*. 2015;*17*:31427–31433.

How to cite this article: Sakti AW, Nishimura Y, Nakai H. Recent advances in quantum-mechanical molecular dynamics simulations of proton transfer mechanism in various water-based environments. *WIREs Comput Mol Sci*. 2019;e1419. https://doi.org/10.1002/wcms.1419